arXiv:0905.2293v1 [math.DS] 14 May 2009

Classification of Complex Polynomial Vector Fields in One Complex Variable

Bodil Branner and Kealey Dias

May 14, 2009

Dedicated to Bob Devaney on his 60^{th} birthday,
and dedicated to the memory of Adrien Douady.

Abstract

The global characterization of structurally stable monic and centered complex polynomial vector fields presented in [DES] is extended to include all monic and centered complex polynomial vector fields in $\mathbb{C}$.

1 History/Motivation

There are various motivations for the study of holomorphic vector fields. These motivations are largely interconnected, but there seem to be three schools of focus which we outline below.

The first school of focus we will mention is that which concentrates on the use of holomorphic vector fields to obtain results within iterative holomorphic dynamics, specifically in studying parabolic bifurcations [Ben93], [Shi00], [Oud99], [BT07], [Eps] and in the proof that there exist Julia sets of positive Lebesgue measure [BC06].

The second school and the one this paper belongs to is studying holomorphic vector fields in their own right (classification) [BT76], [DES], and in the study of quadratic differentials [Jen58], [Str84]. Quadratic differentials and holomorphic vector fields can both be viewed as foliations with singularities. However, the leaves are canonically oriented in the latter case and not in the first.

The last school of focus we will mention is the one that utilizes the integrability of holomorphic vector fields to study real vector fields and continuous dynamical systems. More specifically, limit cycles and inverse problems relating to Hilbert's 16^{th} problem which (among other things) considers the upper bound of the number of limit cycles that can occur for real polynomial vector fields in the plane [Sve78], [Sve81], [Ben91]; Hamiltonian systems [Sve78]; and the existence of centers [Nee94] are studied. Although no limit cycles exist for holomorphic vector fields, an important strategy when dealing with Hilbert's

---

2000 Mathematics Subject Classification: 37F75, 37C15, 37F20.

Keywords and phrases: holomorphic vector field, polynomial vector field, global conjugacy classification, combinatorial invariant, analytic invariant.

16^{th} problem is to study perturbations of holomorphic vector fields with centers [AGP09], [LS04].

In [BT76], the authors use "two numerical invariants" (one being the multiplicity of the zero, and the other coinciding with the *dynamical residue* defined in Section 4 of this paper) associated with the analytic function defining the vector field, which "classify the induced flow up to conformal equivalence." However, this is a local, not global, result. In this vein, [BT76] and [GGJ04] also give the local normal forms for such flows.

Partial results for the global classification of complex polynomial vector fields go back to the classification of quadratic differentials having poles of order ≥ 2 [Jen58], [Str84]. The main case where classification of the global structure of quadratic differentials that applies to holomorphic vector fields is only a classification for given quadratic differentials. When it comes to proving existence of a quadratic differential with prescribed combinatorial and analytic properties (for instance, the so-called "moduli problem" for quadradic differentials with closed trajectories [Str84]), the full classification of vector fields is excluded since these theorems are only applicable to a special subclass of vector fields, or they assume a finite area condition, which holomorphic vector fields with at least one zero never satisfy. Muciño-Raymundo [MR02] studies vector fields but also only covers a specific class.

The study of global classification for complex polynomial vector fields in $\mathbb{C}$ is recent [DES], and is formulated as follows.

The global characterization of a monic, centered complex polynomial vector field corresponding to a fixed polynomial P is determined by a *combinatorial data set* (describing the topology) and an *analytic data set* (describing the geometry). These invariants uniquely describe such a vector field. That is, two monic and centered polynomial vector fields with the same invariants must be identical, and given a set of invariants, there exists a unique monic, centered polynomial vector field having those invariants.

Douady, Estrada, and Sentenac [DES] classified the *structurally stable*[1] case, i.e. the vector fields such that there are neither homoclinic separatrices nor multiple equilibrium points. It will be shown in [DT] that these vector fields in fact make up an open and dense subset of full dimension in parameter space.

In this paper, we complete the classification of the global structure of complex polynomial vector fields in $\mathbb{C}$ by extending the result in [DES] to include the non-structurally stable vector fields.

The contents of this paper are as follows.

In Section 2, we review the basic definitions and results of monic centered polynomial vector fields in $\mathbb{C}$ for polynomials of a fixed degree $d \geq 2$. Sections 3 and 4 contain the definitions of the combinatorial and the analytic invariants of such a given vector field and synthesize their properties so that we are able to abstractly define combinatorial and analytic data sets. In Section 5 we show that two polynomial vector fields with the same invariants are identical, and also that any two polynomial vector fields in the same combinatorial class have quasi-conformally equivalent flows. In Sections 6 - 10, the invariants are proven to be realizable, formulated in Section 6 as the main theorem, the *Structure Theorem*[2], which is proven in several steps in the sections that follow.

---

[1] Called *generic* in [DES]

[2] Note that the *Structure Theorem* in Jenkins [Jen58] is a different statement.

From any given combinatorial and analytic data set we construct in Section 7 a Riemann surface $\mathcal{M}$, called the *rectified surface*. In Section 8 it is shown to be isomorphic to the Riemann sphere $\hat{\mathbb{C}}$. The manifold $\mathcal{M}$ is obtained from an open non-compact Riemann surface $\mathcal{M}^*$ as the compactification of $\mathcal{M}^*$ by adding a number of points determined by the combinatorial data set. By construction, $\mathcal{M}^*$ has a canonical vector field $\xi_{\mathcal{M}}$ assigned. In Section 9, this vector field is shown to extend continuously to the zero vector at all the added points, identifying the equilibrium points of $\xi_{\mathcal{M}}$. In the final Section 10, we show the existence of a unique biholomorphism $\Phi : \mathcal{M} \to \hat{\mathbb{C}}$, which makes the vector field $\Phi_*(\xi_{\mathcal{M}})$ a polynomial vector field realizing the given combinatorial and analytic invariants. The combinatorial and analytic data sets therefore give a complete global classification of polynomial vector fields.

Acknowledgements. We are indebted to Adrien Douady for suggesting the research topic. We would like to thank Douady and likewise Pierette Sentenac for several helpful conversations about their work on the topic. In addition, we want to thank Christian Henriksen for helpful comments and suggestions and Xavier Buff for the suggestion of using Fatou coordinates in Subsection 7.4.

2 Introduction/Preliminaries/Definitions

We recall now some general concepts. Details for much of this section can be found in [DES] and [BT76].

Given P in $\mathcal{P}_d$, the set of monic and centered polynomials of degree $d \geq 2$, there is an associated vector field $\xi_P \in \Xi_d$ where $\xi_P(z) = P(z)\frac{d}{dz}$. Such a vector field has a corresponding differential equation

$$\dot{z} = P(z), \tag{1}$$

where $\dot{z} = \frac{dz}{dt}$, $t \in \mathbb{R}$. The vector field ξ_P has equilibrium points ζ at the roots of P, i.e. $P(\zeta) = 0$. There are four types of equilibrium points: three types correspond to simple roots of P, and one type corresponds to multiple roots of P.

Definition 2.1. An equilibrium point ζ is a *sink*, *source*, or *center* if and only if $P(\zeta) = 0$, $P'(\zeta) \neq 0$, and $\Re(P'(\zeta))$ is negative, positive, or zero respectively. An equilibrium point ζ is a *multiple equilibrium point* of multiplicity m if and only if $P(\zeta) = 0$, $P'(\zeta) = \cdots = P^{(m-1)}(\zeta) = 0$, and $P^{(m)}(\zeta) \neq 0$.

The *maximal solution* $\gamma(t, z_0)$ of Equation (1) through z_0 at $t = 0$ satisfies $\gamma(0, z_0) = z_0$ and $\gamma'(t, z_0) = P(\gamma(t, z_0))$ for each t in the maximal interval $]t_{min}, t_{max}[$ where $t_{min} \in \mathbb{R}_- \cup \{-\infty\}$ and $t_{max} \in \mathbb{R}_+ \cup \{+\infty\}$. The image $\gamma(]t_{min}, t_{max}[, z_0)$ is the *trajectory* through z_0. If z_0 is not an equilibrium point and if the maximal interval of $\gamma(\cdot, z_0)$ is mapped bijectively onto the trajectory through z_0, then the limit points of the trajectory are as follows.

- For $t_{min} = -\infty$: $\lim\limits_{t\to-\infty} \gamma(t, z_0) = \zeta_\alpha$, a source or a multiple equilibrium point.
- For $t_{max} = +\infty$: $\lim\limits_{t\to+\infty} \gamma(t, z_0) = \zeta_\omega$, a sink or a multiple equilibrium point.

- For $t_{min} < 0$: $\lim\limits_{t \to t_{min}} \gamma(t, z_0) = \infty$,
  the point at infinity
- For $t_{max} > 0$: $\lim\limits_{t \to t_{max}} \gamma(t, z_0) = \infty$,
  the point at infinity.

If z_0 is not an equilibrium point and if the maximal interval of $\gamma(\cdot, z_0)$ is not mapped bijectively onto the trajectory through z_0, then the maximal interval is $\mathbb{R}$ and $\gamma(\cdot, z_0)$ is periodic of period τ where $\tau > 0$ is minimal such that $\gamma(t + \tau, z_0) = \gamma(t, z_0)$, for all $t \in \mathbb{R}$. The bounded component of the complement $\mathbb{C} \setminus \gamma(\mathbb{R}, z_0)$ of the maximal trajectory through z_0 contains a center ζ. The period τ satisfies

$$\tau = \begin{cases} 2\pi i \frac{1}{P'(\zeta)} & \text{if } \Im P'(\zeta) > 0 \\ -2\pi i \frac{1}{P'(\zeta)} & \text{if } \Im P'(\zeta) < 0, \end{cases} \tag{2}$$

where in the first case, ζ is on the left of the periodic trajectory, and in the second case, on the right.

The basins of equilibrium points are defined by the following:

- ζ source:
  $\mathcal{B}(\zeta) = \{z \in \mathbb{C} \mid \gamma(t, z) \to \zeta \text{ for } t \to -\infty\}$
- ζ sink:
  $\mathcal{B}(\zeta) = \{z \in \mathbb{C} \mid \gamma(t, z) \to \zeta \text{ for } t \to +\infty\}$
- ζ center:
  $\mathcal{B}(\zeta) = \{\zeta\} \cup \{z \in \mathbb{C} \mid \gamma(\cdot, z)$ periodic and ζ is in the bounded component of $\mathbb{C} \setminus \gamma(\mathbb{R}, z)\}$
- ζ multiple equilibrium point:

$$\begin{aligned} \mathcal{B}(\zeta) &= \mathcal{B}_\alpha(\zeta) \cup \mathcal{B}_\omega(\zeta) \cup \{\zeta\} \quad \text{where} \\ \mathcal{B}_\alpha(\zeta) &= \{z \neq \zeta \mid \gamma(t, z) \to \zeta \text{ for } t \to -\infty\} \quad \text{is the repelling basin} \\ \mathcal{B}_\omega(\zeta) &= \{z \neq \zeta \mid \gamma(t, z) \to \zeta \text{ for } t \to +\infty\} \quad \text{is the attracting basin.} \end{aligned} \tag{3}$$

The connected components of $\mathcal{B}_\alpha(\zeta)$ and $\mathcal{B}_\omega(\zeta)$ are called *repelling petals* and *attracting petals* respectively. In all four cases, $\mathcal{B}(\zeta)$ is an open, simply-connected domain.

If either t_{min} or t_{max} is finite, then the trajectory associated with this maximal interval is unbounded. It is interesting to study the behavior of a polynomial vector field in a neighborhood of infinity. We state a result from [DES].

Proposition 2.2 (From Chapter I in [DES])**.** *For every polynomial $P \in \mathcal{P}_d$, there exists a unique isomorphism, tangent to the identity at infinity, which conjugates the vector field ξ_P to $\xi_0(z) = z^d \frac{d}{dz}$ in a neighborhood of ∞.*

Another result from [DES] states

Proposition 2.3 (From Chapter I in [DES])**.** *There exist $2d - 2$ solutions γ_ℓ, $\ell \in \{0, 1, \dots, 2d-3\}$ such that*

- *for ℓ odd, γ_ℓ is defined for $]-\alpha_\ell, 0]$ and $|\gamma_\ell(t)| \to \infty$ as $t \to -\alpha_\ell$, and*

- *for ℓ even, γ_ℓ is defined for $[0, \beta_\ell[$ and $|\gamma_\ell(t)| \to \infty$ as $t \to \beta_\ell$.*

In a neighborhood V_∞ of infinity, the trajectory γ_ℓ is asymptotic to the ray $t\delta_\ell$, $t \in \mathbb{R}_+$ determined by δ_ℓ at ∞, where

$$\delta_\ell = \exp\left(2\pi i \frac{\ell}{2(d-1)}\right), \quad \ell \in \{0, 1, \ldots, 2d-3\}. \tag{4}$$

Definition 2.4. The *separatrices* s_ℓ, $\ell = 0, \ldots, 2d-3$, of ξ_P at infinity are the maximal trajectories of ξ_P that have asymptotic directions δ_ℓ at infinity. For ℓ odd, the separatrix is called *outgoing*, and for ℓ even, the separatrix is called *incoming.*

Remark 2.5. Note the labelling of the separatrices which will be important, among other things, for the uniqueness in the Structure Theorem 10.1.

There are two possibilities for a separatrix s_ℓ. Either it is *landing*, or it is *homoclinic.*

Definition 2.6. We say s_ℓ is *landing* or s_ℓ *lands* at ζ in $\mathbb{C}$ if $\zeta = \bar{s}_\ell \setminus s_\ell$ is the limit point of s_ℓ in $\mathbb{C}$ as t tends to $+\infty$ or $-\infty$, depending on whether s_ℓ is an outgoing or incoming separatrix to the point at infinity.

The limit point ζ is a sink, source, or multiple equilibrium point.

Definition 2.7. If $\bar{s}_\ell \setminus s_\ell = \emptyset$ in $\mathbb{C}$, then the separatrix is both outgoing from and incoming to infinity, and is called a *homoclinic separatrix* of infinity.

Remark 2.8 (Remark and Notation)**.** When we need to specify that ℓ is even or odd, we use j and k respectively, while ℓ is used to denote either even or odd.

Homoclinic separatrices will sometimes be notated by $s_{k,j}$ with two indices, one odd and one even to specify both the outgoing and incoming directions it has at infinity.

We will often consider ξ_P on the Riemann sphere $\hat{\mathbb{C}}$, where infinity is a pole of order $d-2$ (see [DES]).

Definition 2.9. The *separatrix graph* of ξ_P is

$$\Gamma_P = \bigcup_{\ell=0}^{2d-3} \hat{s_\ell}, \tag{5}$$

where $\hat{s}_\ell$ is the closure in $\hat{\mathbb{C}}$.

Remark 2.10. The separatrix graph Γ_P contains infinity and *all* sinks, sources, and multiple equilibrium points, but not centers. That is, for every equilibrium point which is not a center, there exists at least one separatrix which lands at it.

The connected components Z of $\hat{\mathbb{C}} \setminus \Gamma_P$ are called *zones.* Note that every separatrix is on the boundary of one or two zones (for proof, see [DES]). Within the zones, all maximal solutions are defined on all of $\mathbb{R}$. The following two propositions characterize their types, and it is important to note that the types of zones are determined by the types of their boundaries.

Proposition 2.11. *Trajectories in a zone Z that contains an equilibrium point are periodic, and the equilibrium point is a center. In this case Z is called a* center zone*. The boundary of a center zone consists of one or several homoclinic separatrices and the point at infinity.*

Proof. See [DES] and, for instance, [Nee94]. $\square$

Otherwise, a zone does not contain an equilibrium point in its interior and has at least one equilibrium point on the boundary ∂Z. In such a zone, each solution has an α-limit point ζ_α and an ω-limit point ζ_ω [DES].

Proposition 2.12 (From Chapter I in [DES])**.** *Trajectories in a zone that does not contain equilibrium points have a common α-limit point ζ_α and a common ω-limit point ζ_ω. From this, one can deduce two types of zones not having an equilibrium point in its interior.*

1. *There are exactly two equilibrium points on ∂Z, i.e. $\zeta_\alpha \neq \zeta_\omega$. In this case, Z is called an* $\alpha\omega$-zone *and is of four subtypes:*
   - $Z = \mathcal{B}(\zeta_\alpha) \cap \mathcal{B}(\zeta_\omega)$, *where ζ_α and ζ_ω are a source and a sink respectively.*
   - $Z = \mathcal{B}(\zeta_\alpha) \cap \mathcal{B}_\omega(\zeta_\omega)$, *where ζ_α and ζ_ω are a source and a multiple equilibrium point respectively. In this case, Z is called an* attracting interpetal *for ζ_ω.*
   - $Z = \mathcal{B}_\alpha(\zeta_\alpha) \cap \mathcal{B}(\zeta_\omega)$, *where ζ_α and ζ_ω are a multiple equilibrium point and a sink respectively. In this case, Z is called a* repelling interpetal *for ζ_α.*
   - $Z = \mathcal{B}_\alpha(\zeta_\alpha) \cap \mathcal{B}_\omega(\zeta_\omega)$, *where ζ_α and ζ_ω are both multiple equilibrium points. In this case, Z is a repelling interpetal for ζ_α and an attracting interpetal for ζ_ω.*

   The boundary ∂Z contains one or two incoming separatrices and one or two outgoing separatrices, and possibly one or several homoclinic separatrices.

2. *There is exactly one equilibrium point on ∂Z, i.e. $\zeta_\alpha = \zeta_\omega$. This case corresponds necessarily to a multiple equilibrium point:*
   - $Z = \mathcal{B}_\alpha(\zeta) \cap \mathcal{B}_\omega(\zeta)$ *and is called a* sepal zone *or just* sepal*. There are exactly $2m-2$ sepals corresponding to a multiple equilibrium point of multiplicity m (see [DES] for details).*

   The boundary ∂Z contains exactly one incoming and one outgoing separatrix and posssibly one or several homoclinic separatrices.

The point at infinity is a boundary point for each zone. Within each zone, there are one or several accesses to infinity.

Definition 2.13. The $2d-2$ *ends at infinity* are the *principal points* of the $(2d-2)$ prime ends at infinity, defined by the accesses to infinity, where *prime end* is in the sense of Carathéodory.

The ends e_ℓ are numbered according to their accessibility; the end e_ℓ has access between the separatrices $s_{\ell-1}$ and s_ℓ.

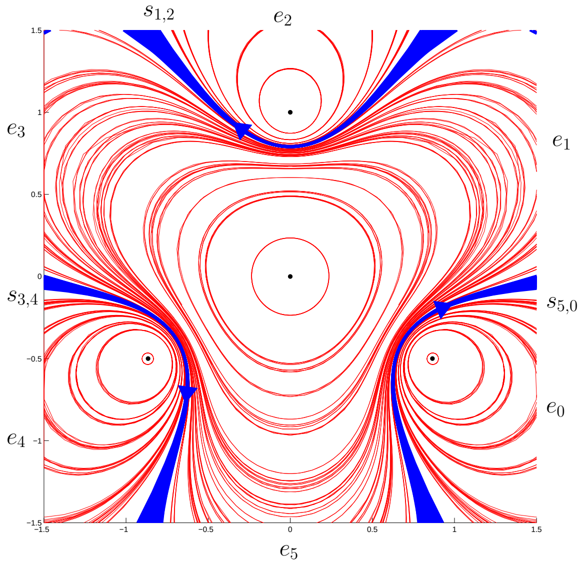

Figure 1: An example of the trajectories of a monic and centered polynomial vector field with a counter-clockwise center zone having three homoclinic separatrices $s_{5,0}$, $s_{1,2}$, and $s_{3,4}$ and three odd ends e_1, e_3, and e_5 on the boundary.

Proposition 2.14 (Characterization of the ends on the boundary of zones)**.**

- *If a center zone Z has n homoclinic separatrices on the boundary ∂Z, then the center zone has n ends at infinity on ∂Z. The ends are all odd if the center zone is to the left of the oriented homoclinic separatrices and all even if the center zone is to the right. In these cases, the zones are called* counter-clockwise *and* clockwise *(or sometimes* odd *and* even*) center zones respectively (see Figure 1).*

- *If a sepal zone Z has n homoclinic separatrices on the boundary ∂Z, then the sepal zone has $n+1$ ends at infinity on ∂Z. They are all odd if the sepal zone is to the left of the oriented homoclinic separatrices and all even if the sepal zone is to the right. In these cases, the zones are called* odd *and* even *sepal zones respectively (see Figure 2).*

- *If an $\alpha\omega$-zone Z is both on the left of n^+ homoclinic separartrices on ∂Z and on the right of n^- homoclinic separatrices on ∂Z, then the $\alpha\omega$-zone has $n^+ + 1$ odd ends and $n^- + 1$ even ends on its boundary ∂Z (see Figure 3).*

Remark 2.15 (Notation)**.** When we want to distinguish between the different types of zones, we denote an $\alpha\omega$-zone by $Z^{\alpha\omega}$, a center zone by Z^c, and a sepal zone by Z^s.

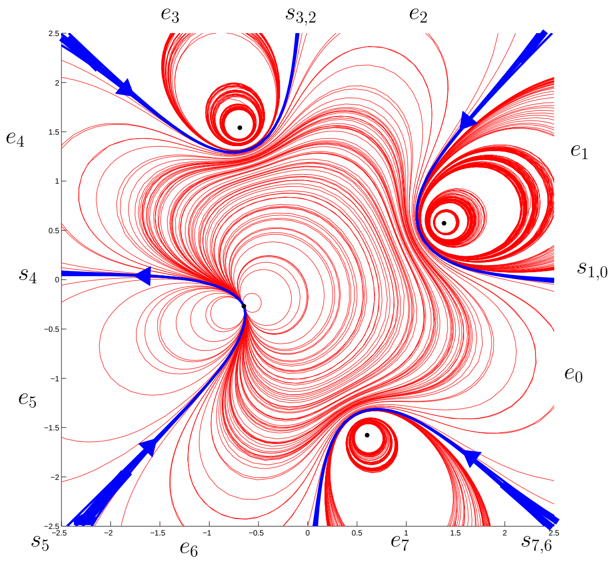

Figure 2: An example of the trajectories of a monic and centered polynomial vector field with one odd sepal zone with one end e_5 on the boundary and one even sepal zone with three homoclinic separatrices $s_{1,0}$, $s_{3,2}$, and $s_{7,6}$ and four even ends e_0, e_2, e_4, and e_6 on the boundary.

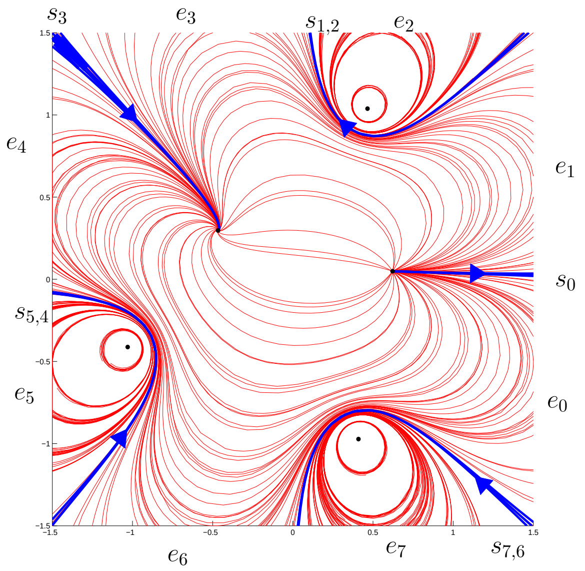

Figure 3: An example of the trajectories of a monic and centered polynomial vector field with an $\alpha\omega$-zone $Z_{3,0}^{\alpha\omega}$ having one clockwise homoclinic separatrix $s_{1,2}$, two counter-clockwise homoclinic separatrices $s_{5,4}$ and $s_{7,6}$, two odd ends e_1 and e_3, and three even ends e_0, e_4, and e_6 on the boundary.

2.1 Numbering conventions

We now want to be able to label the homoclinic separatrices and zones with an index that contains some combinatorial information. There are several ways to do this, but we use the following conventions.

Let $h_P \geq 0$ be the number of homoclinic separatrices for ξ_P, and let k be the uniquely determined odd number so that $s = s_{k,j}$. We number the homoclinic separatrices by $s_{k_1,j_1}, \ldots, s_{k_{h_P},j_{h_P}}$ such that

$$0 < k_1 < \cdots < k_{h_P} \leq 2d - 3. \tag{6}$$

Let $Z^{\alpha\omega}$ be an $\alpha\omega$-zone for ξ_P. From Theorem 2.12, we know that $Z^{\alpha\omega}$ has at least one incoming (even) landing separatrix and at least one outgoing (odd) landing separatrix on $\partial Z^{\alpha\omega}$. We label $Z^{\alpha\omega}_{k,j}$ by the landing separatrix s_k outgoing from the odd end e_k and the landing separatrix s_j incoming to the even end e_j on $\partial Z^{\alpha\omega}$. Let $s_P \geq 0$ be the number of $\alpha\omega$-zones. We number the zones $Z^{\alpha\omega}_{k_1,j_1}, \ldots, Z^{\alpha\omega}_{k_{s_P},j_{s_P}}$ corresponding to

$$0 \leq j_1 < \cdots < j_{s_P} < 2d - 3. \tag{7}$$

We label an odd sepal-zone for ξ_P by Z^s_k, where s_k is the unique odd landing separatrix on the boundary. Let n^+_s be the number of odd sepal-zones. We number the zones $Z^s_{k_1}, \ldots, Z^s_{k_{n^+_s}}$ corresponding to

$$0 < k_1 < \cdots < k_{n^+_s} \leq 2d - 3. \tag{8}$$

We label an even sepal-zone for ξ_P by Z^s_j, where s_j is the unique even landing separatrix on the boundary. Let n^-_s be the number of even sepal-zones. We number the zones $Z^s_{j_1}, \ldots, Z^s_{j_{n^-_s}}$ corresponding to

$$0 \leq j_1 < \cdots < j_{n^-_s} < 2d - 3. \tag{9}$$

We label an odd center-zone for ξ_P by Z^c_k, where k is the smallest odd index of the homoclinic separatrices on the boundary. Let n^+_c be the number of odd center-zones. We number the zones $Z^c_{k_1}, \ldots, Z^c_{k_{n^+_c}}$ corresponding to

$$0 < k_1 < \cdots < k_{n^+_c} \leq 2d - 3. \tag{10}$$

We label an even center-zone for ξ_P by Z^c_j, where j is the smallest even index of the homoclinic separatrices on the boundary. Let n^-_c be the number of even center-zones. We number the zones $Z^c_{j_1}, \ldots, Z^c_{j_{n^-_c}}$ corresponding to

$$0 \leq j_1 < \cdots < j_{n^-_c} < 2d - 3. \tag{11}$$

Theorem 2.16 (from [DES])**.** *For a given vector field $\xi_P \in \Xi_d$, there exist holomorphic isomorphisms ϕ*

- *from each $\alpha\omega$-zone $Z^{\alpha\omega}_{k,j}$ to a horizontal strip $\Sigma_{k,j}$, where j is the index of the separatrix s_j described above whose image is on the upper boundary of the strip $\Sigma_{k,j}$ and k is the index of the separatrix s_k described above whose image is on the lower boundary (see Figure 13).*

- *from each odd sepal zone Z_k^s to an upper half plane $\mathbb{H}_k$ and from each even sepal zone Z_j^s to a lower half plane $-\mathbb{H}_j$,*
- *and from each center zone minus the curve $\overline{\gamma}_e$, which is orthogonal to the periodic trajectories in Z^c and joins the center ζ and ∞ through the access defining e, to a vertical half-strip C. For an odd center zone, ϕ maps $Z_k^c \setminus \overline{\gamma}_{e_k}$ to an upper vertical half-strip $C_k = \{z \in \mathbb{H} \mid 0 < \Re(z) < \tau\}$, and for an even center zone, ϕ maps $Z_j^c \setminus \overline{\gamma}_{e_j}$ to a lower vertical half-strip $C_j = \{z \in -\mathbb{H} \mid 0 < \Re(z) < \tau\}$, where τ is the period of the periodic trajectories,*

such that these isomorphisms conjugate ξ_P to $\frac{d}{dz}$.

These isomorphisms take the form

$$\phi(z) = \int_e^z \frac{dw}{P(w)}, \tag{12}$$

where e is one of the ends at infinity on the boundary of the zone.

Remark 2.17. The $Z^{\alpha\omega}$, Z^s, and $Z^c \setminus \overline{\gamma}_e$ are simply connected. Therefore, the integral in (12) is path independent and the function ϕ is well-defined up to addtion by a constant when the end e is changed. The function ϕ is actually well-defined in any simply connected domain which avoids the roots of P.

We then have

$$\phi_*(\xi_P) = \phi'(z)\, P(z)\, \frac{d}{dz} = \frac{d}{dz}. \tag{13}$$

Definition 2.18. The isomorphisms ϕ are called *rectifying coordinates* of $(\mathbb{C}, \xi_P)$.

We elaborate on the structure of the rectified zones $\pm\mathbb{H}_\ell$, $\Sigma_{k,j}$, and C_ℓ.

- For an $\alpha\omega$-zone $Z^{\alpha\omega}$, a branch of ϕ is chosen such that $e := e_{k_0}$ is one of the odd ends on its boundary. Thus, $\phi_{k_0} : e_{k_0} \mapsto 0$, and further all of the odd ends on $\partial Z^{\alpha\omega}$ are mapped to $\mathbb{R}$. Any homoclinic separatrices on $\partial Z^{\alpha\omega}$ connecting two odd ends on $\partial Z^{\alpha\omega}$ are also mapped to $\mathbb{R}$. The one separatrix on $\partial Z^{\alpha\omega}$ incoming to an odd end and the one separatrix on $\partial Z^{\alpha\omega}$ outgoing from an odd end are also mapped to $\mathbb{R}$. All even ends, homoclinic separatrices connecting two even ends, and the separatrices incoming to and outgoing from an even end on $\partial Z^{\alpha\omega}$ have their images on $\mathbb{R} + ih$, where h is the height of the strip.
- For an odd sepal zone Z_k^s, a branch of ϕ is chosen such that $e := e_{k_0}$ is one of the odd ends on its boundary. Thus, $\phi_{k_0} : e_{k_0} \mapsto 0$, $\phi_{k_0} : Z_k^s \to \mathbb{H}_k$, and further all of the odd ends, all homoclinic separatrices, and the two landing separatrices on ∂Z^s are mapped to $\mathbb{R}$.
- For an even sepal zone Z_j^s, a branch of ϕ is chosen such that $e := e_{j_0}$ is one of the even ends on its boundary. Thus, $\phi_{j_0} : e_{j_0} \mapsto 0$, $\phi_{j_0} : Z_j^s \to -\mathbb{H}_j$, and further all of the even ends, all homoclinic separatrices, and the two landing separatrices on ∂Z^s are mapped to $\mathbb{R}$.
- For an odd center zone Z_k^c containing a center ζ, a branch of ϕ is chosen such that $e := e_{k_0}$ is one of the odd ends on its boundary. Thus, $\phi_{k_0} : e_{k_0} \mapsto 0$, $\phi_{k_0} : Z^c \setminus \overline{\gamma}_{e_{k_0}} \to C_{k_0}$, and further all of the odd ends and all homoclinic separatrices on ∂Z_k^c are mapped to $\mathbb{R}$.

- For an even center zone Z^c_j, a branch of ϕ is chosen such that $e := e_{j_0}$ is one of the even ends on its boundary. Thus, $\phi_{j_0} : e_{j_0} \mapsto 0$, $\phi_{j_0} : Z^c \backslash \overline{\gamma}_{e_{j_0}} \to C_{j_0}$, and further all of the even ends and all homoclinic separatrices on ∂Z^c_j are mapped to $\mathbb{R}$.

The images of the ends e_ℓ and separatrices s_ℓ under ϕ are worth distinction and are denoted E_ℓ and S_ℓ respectively.

To each $\alpha\omega$-zone are associated specific curves joining the odd ends to the even ends. It will become clear in the next section that these curves are complementary to homoclinic separatrices in more ways than one. The definition follows.

Definition 2.19 (Transversals)**.** A *transversal* $T_{k,j}$ of ξ_P is a curve joining the ends e_k and e_j, such that it does not cross any separatrices and crosses the trajectories of ξ_P at a constant, non-zero angle.

In rectifying coordinates, the images of the transversals are the straight line segments joining the E_k to the E_j in a strip.

3 Combinatorial Data Set for ξ_P

The goal of this section is to define a *combinatorial data set* which completely describes the topological structure of a vector field $\xi_P \in \Xi_d$.

The separatrices of ξ_P are labeled by the integers $\{0, \ldots, 2d-3\}$ or by elements of $\mathbb{Z}/(2d-2)$ where $0, \ldots, 2d-3$ are our preferred representatives.

The structure of the separatrix graph Γ_P is reflected in an equivalence relation $\sim_P$ on $\mathbb{Z}/(2d-2)$, to be defined below. Such equivalence relations have certain properties that we synthesize into the definiton of a *combinatorial data set of degree d* to be defined in Definition 3.18.

Any $\xi_P \in \Xi_d$ gives rise to a combinatorial data set of degree d, and we will prove in Sections 6-10 that any combinatorial data set is realized by polynomial vector fields from Ξ_d. To a given combinatorial data set of degree d is therefore associated a *combinatorial class* of polynomial vector fields, i.e. all ξ_P realizing the given combinatorial data set.

A combinatorial data set is also called a *combinatorial invariant*.

Definition 3.1. Let $\xi_P \in \Xi_d$ be given. Then the equivalence relation $\sim_P$ and the marked set H_P on $\mathbb{Z}/(2d-2)$ are defined as follows:

1. $H_P \subset \mathbb{Z}/(2d-2)$ is the subset defined by

$$\ell \in H_P \Leftrightarrow s_\ell \text{ is a homoclinic separatrix of } \xi_P$$

2. The equivalence relation $\sim_P$ on $\mathbb{Z}/(2d-2)$ is defined by

$$\text{If } \ell', \ell'' \in H_P, \text{ then } \ell' \sim_P \ell'' \Leftrightarrow s_{\ell'} = s_{\ell''}.$$
$$\text{If } \ell', \ell'' \notin H_P, \text{ then } \ell' \sim_P \ell'' \Leftrightarrow \text{ the separatrices } s_{\ell'} \text{ and } s_{\ell''} \text{ of } \xi_P \text{ land at the same point in } \mathbb{C}.$$

Remark 3.2 (Remark and Notation)**.** It is convenient to use L_P to name the complement of H_P: the set of ℓ such that s_ℓ lands in $\mathbb{C}$.

We sometimes represent L_P and H_P by a symbolic disk representation (see Figure 4) where we draw the asymptotic directions of the separatrices on $\mathbb{S}^1$ and draw in curves with arrows representing the separatrices. We also add points corresponding to equilibrium points and sometimes transversals.

For ξ_P given and $[\ell] \subseteq L_P$ an equivalence class of $\sim_P$, the equilibrium point which is the common landing point of $s_{\ell'}$ for $\ell' \in [\ell]$ is denoted $\zeta_{[\ell]}(\xi_P)$ or $\zeta_{[\ell]}$ when the vector field is clear from the context.

Definition 3.3. For ξ_P given, an equivalence class $[\ell] \subseteq L_P$ is called *odd*, *even*, or *mixed* if and only if it consists respectively of only odd elements, only even elements, or both odd and even elements (denoted respectively by $[k]$, $[j]$, and $[m]$). An equivalence class $[\ell] \subseteq H_P$ consists of exactly two integers, one even and one odd and is called *homoclinic*.

Note that $\sim_P$ has one equivalence class if and only if $P(z) = z^d$.

Remark 3.4 (Notation)**.** We use $I = [\ell', \ell'']$ to denote the interval in $\mathbb{Z}/(2d-2)$ consisting of all the elements $\ell', \ell'+1, \ldots, \ell''-1, \ell''$ (i.e. in the counter-clockwise direction). With the preferred representatives $0, \ldots, 2d-3$, it is possible to have $\ell'' < \ell'$, in which case $0 \in I$.

Definition 3.5. We define the *shift map* $\sigma : \mathbb{Z}/(2d-2) \to \mathbb{Z}/(2d-2)$ for $H_P \cup L_P$ so that it is a bijection on each equivalence class $[\ell]$ and defined by $\sigma(\ell)$ giving the next label in the equivalence class in the counter-clockwise direction and $\sigma^{-1}(\ell)$ giving the next in the clockwise direction with respect to the asymptotic directions δ_ℓ.

The mapping σ is an involution on H_P, i.e. for $k \in H_P$, $k \sim_P j$, $\sigma(k) = j$ and $\sigma(j) = k$.

Remark 3.6 (Notation)**.** For an equivalence class $[\ell] \subset L_P$, we denote by $p_{[\ell]}$ the number of parity changes

$$p_{[\ell]} = \begin{cases} 0 & \text{if } [\ell] = [k] \text{ or } [j] \\ \sum\limits_{\ell' \in [m]} 2\left(\left\lfloor \frac{\sigma(\ell')-\ell'}{2} \right\rfloor - \frac{\sigma(\ell')-\ell'}{2}\right) & \text{if } [\ell] = [m] \end{cases}. \tag{14}$$

That is, we count each time $\sigma(\ell') - \ell'$ is odd.

The number $p_{[\ell]}$ of parity changes (corresponding to the number of sepals for $\zeta_{[\ell]}$) is always even, and the number of times there is a change from odd to even is equal to the number of changes from even to odd.

For $\sim_P$, $\sum\limits_{[\ell] \subseteq L_P} p_{[\ell]}$ corresponds to the total number of sepals for the vector field. For $\sim_P$ and $[m]$ a mixed equivalence class, the number of interpetals (recall Proposition 2.12) is equal to the number of times the parity does not change, i.e. when $\sigma(\ell) - \ell$, $\ell \in [m]$ is even. The interpetal is attracting when two adjacent elements in $[m]$ are odd, and the interpetal is repelling when two adjacent elements are even.

Definition 3.7 (Non-crossing equivalence relation)**.** An equivalence relation $\sim$ is non-crossing if and only if, for any equivalence classes $[\ell]$ with arbitrary $\ell', \ell'' \in [\ell]$, any other equivalence class $[\tilde{\ell}]$ is contained in either $[\ell'+1, \ell''-1]$ or $[\ell''+1, \ell'-1]$.

Note that the equivalence relation $\sim_P$ associated to a vector field ξ_P is non-crossing since the separatrices of ξ_P are non-crossing.

Important structures induced by the equivalence relation on H_P are H_P-*chains.*

Definition 3.8. A set $\{[k_{i_q}]\} \subseteq H_P$ of $n \geq 1$ distinct equivalence classes such that $\{i_q \mid q = 1, \ldots, n\} \subseteq \{1, \ldots, h_P\}$ forms a *counter-clockwise closed H_P-chain of length n* if

$$\begin{aligned} k_{i_q} &= \sigma\left(k_{i_{q-1}}\right) + 1, \quad q = 2, \ldots, n \\ k_{i_1} &= \sigma\left(k_{i_n}\right) + 1 \end{aligned} \tag{15}$$

or forms a *clockwise closed H_P-chain of length n* if for $j_{i_q} = \sigma\left(k_{i_q}\right)$

$$\begin{aligned} j_{i_q} &= \sigma\left(j_{i_{q-1}}\right) + 1, \quad q = 2, \ldots, n \\ j_{i_1} &= \sigma\left(j_{i_n}\right) + 1 \end{aligned} \tag{16}$$

Definition 3.9. A set $\{[k_{i_q}]\} \subseteq H_P$ of $n \geq 0$ distinct equivalence classes such that $\{i_q \mid q = 1, \ldots, n\} \subseteq \{1, \ldots, h_P\}$ forms a *counter-clockwise open H_P-chain of length n* if for $j_{i_q} = \sigma\left(k_{i_q}\right)$

$$\begin{aligned} k_{i_q} &= \sigma\left(k_{i_{q-1}}\right) + 1, \quad q = 2, \ldots, n \\ k_{i_1} - 1,\, \sigma\left(k_{i_n}\right) + 1 &\notin H_P \end{aligned} \tag{17}$$

or forms a *clockwise open H_P-chain of length n* if

$$\begin{aligned} j_{i_q} &= \sigma\left(j_{i_{q-1}}\right) + 1, \quad q = 2, \ldots, n \\ j_{i_1} - 1,\, \sigma\left(j_{i_n}\right) + 1 &\notin H_P. \end{aligned} \tag{18}$$

Note that any equivalence class $\{k, j\} \subseteq H_P$ is part of a unique counter-clockwise (open or closed) H_P-chain and of a unique clockwise (open or closed) H_P-chain.

The H_P-chains are natural structures if one looks at the boundary components of the rectified zones.

The homoclinic separatrices corresponding to a closed counter-clockwise (clockwise) H_P-chain form the boundary in $\mathbb{C}$ of a counter-clockwise (clockwise) center zone (see Figure 4). In rectifying coordinates, the homoclinic separatrices lie on the lower (upper) boundary of the vertical half-strip. The separatrices corresponding to an open counter-clockwise (clockwise) H_P-chain are part of the boundary in $\mathbb{C}$ of an odd (even) sepal zone or an $\alpha\omega$-zone (see Figure 5). In rectifying coordinates, the separatrices lie on the lower (upper) boundary of the half-plane or the strip.

Let $H_{\{[k_{i_1}]\}}$ denote a counter-clockwise H_P-chain and $H_{\{[j_{i_1}]\}}$ be a clockwise H_P-chain, where it will be specified whether it is open or closed when needed. We label the length $n_{\{[\ell_{i_1}]\}}$ by the chain it is associated to, but we sometimes use only n^+ or n^- for counter-clockwise and clockwise respectively, or sometimes n for ease in notation when the context is clear.

Complementary to the H_P-chains are the structures induced by the transversals. Let

$$T_P = \{(k, \sigma(k-1)) \mid \sigma(k-1) - (k-1) \in 2\mathbb{Z}\} \cup \{(\sigma(j-1), j) \mid \sigma(j-1) - (j-1) \in 2\mathbb{Z}\}. \tag{19}$$

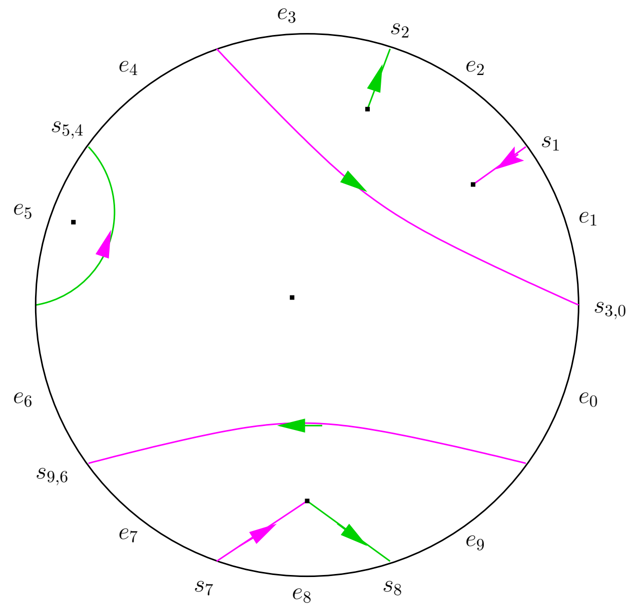

Figure 4: Example of a disk representation for some $\xi_P \in \Xi_6$ containing one counter-clockwise closed H_P-chain $H_{\{[5]\}}$, one clockwise closed H_P-chain $H_{\{[0]\}}$, and two counter-clockwise open H_P-chains $H_{\{[3]\}}$ and $H_{\{[9]\}}$.

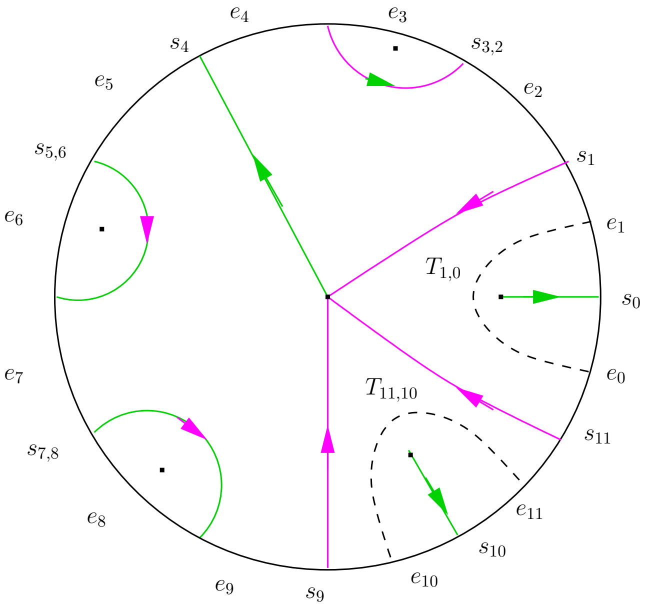

Figure 5: Example of a disk representation for some $\xi_P \in \Xi_7$ containing one counter-clockwise open H_p-chain $H_{\{[5]\}}$, one clockwise open H_P-chain $H_{\{[2]\}}$, and two clockwise open T_P-chains $T_{\{[1]\}}$ and $T_{\{[11]\}}$.

Definition 3.10. The *essential transversals* are the transversals $T_{k,j}$ such that $(k,j) \in T_P$. Any other transversal will be called a *non-essential transversal* (see Figure 9).

Remark 3.11. Note that in an $\alpha\omega$-zone $Z_{k,j}^{\alpha\omega}$, the essential transversals are the transversals $T_{\sigma^{-1}(j)+1,j}$ and $T_{k,\sigma^{-1}(k)}$ (see Figure 9). Note that $T_{\sigma^{-1}(j)+1,j} = T_{k,\sigma^{-1}(k)}$ if and only if there are no homoclinic separatrices on the boundary of $Z_{k,j}^{\alpha\omega}$.

The structures complementary to the H_P-chains are based on these essential transversals and are called *transversal chains* or *T_P-chains*, defined below.

Definition 3.12. A set of $n \geq 1$ distinct transversals T_{k_i,j_i} such that $(k_i,j_i) \in T_P$, $i = 1, ..., n$, form a *counter-clockwise closed T_P-chain of length n* if

$$\begin{aligned} k_i &= j_{i-1} + 1, \quad i = 2, ..., n \\ k_1 &= j_n + 1 \end{aligned} \tag{20}$$

or forms a *clockwise closed T_P-chain of length n* if

$$\begin{aligned} j_i &= k_{i-1} + 1, \quad i = 2, ..., n \\ j_1 &= k_n + 1 \end{aligned} \tag{21}$$

Definition 3.13. A set of $n \geq 1$ distinct transversals T_{k_i,j_i} such that $(k_i,j_i) \in T_P$, $i = 1, ..., n$, form a *counter-clockwise open T_P-chain of length n* if

$$\begin{gathered} k_i = j_{i-1} + 1, \quad i = 2, ..., n \\ (\cdot, k_1 - 1) \cap T_P = \emptyset, \text{ and } (j_n + 1, \cdot) \cap T_P = \emptyset \end{gathered} \tag{22}$$

or forms a *clockwise open T_P-chain of length n* if

$$\begin{gathered} j_i = k_{i-1} + 1, \quad i = 2, ..., n \\ (j_1 - 1, \cdot) \cap T_P = \emptyset, \text{ and } (\cdot, k_n + 1) \cap T_P = \emptyset \end{gathered} \tag{23}$$

If an equilibrium point is contained in a component of $\mathbb{C} \setminus \{T_{k,j} \mid (k,j) \in T_P\}$ having a counter-clockwise closed T_P-chain on the boundary, it is a source. If an equilibrium point is contained in a component having a clockwise closed T_P-chain on the boundary, it is a sink (see Figure 9). So to each closed T_P-chain is an associated equivalence class $[\ell]$ corresponding to the equilibrium point $\zeta_{[\ell]}$, even for counter-clockwise, odd for clockwise. When a multiple equilibrium point has an interpetal (which is true in all but the case $P(z) = z^d$), then there will be open T_P-chains on the boundary. Let $T_{\{[k_{i_1}]\}}$ denote a counter-clockwise T_P-chain and $T_{\{[j_{i_1}]\}}$ be a clockwise T_P-chain, where it will be specified whether it is open or closed when needed (see Figures 6, 7, and 8). We label the length as for the H_P-chains.

For a multiple equilibrium point, there are some open H_P-chains together with some open T_P-chains that form the boundary of a domain containing all (and only) the separatrices landing at the multiple equilibrium point (see Figure 5).

The set $\mathbb{Z}/(2d-2)$ has a natural geometric representation as the marked points (later called *division points*) $\delta_\ell = \exp\left(\frac{2\pi i \ell}{2d-2}\right)$ on the unit circle $\mathbb{S}^1$. For

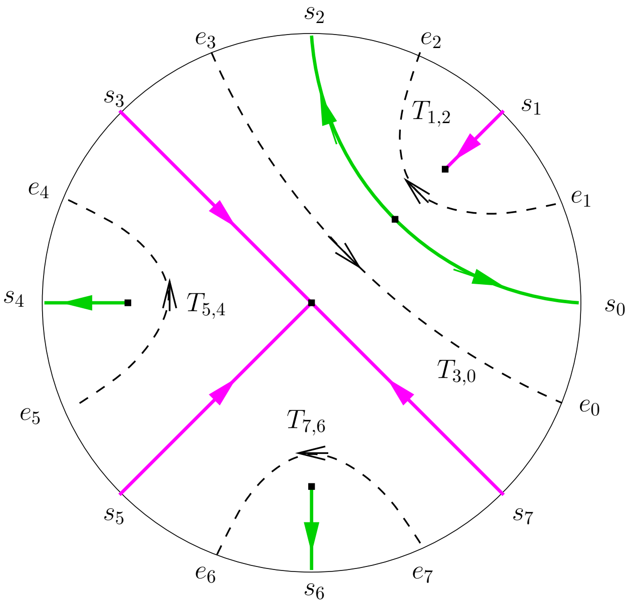

Figure 6: Example of a disk representation of a vector field ξ_P of degree $d = 5$ having neither multiple equilibrium points nor homoclinic separatrices. The transversals are all essential and represented by the dashed lines, and their orientations are denoted by the arrows. Figures 7 and 8 depict the corresponding transversal chains in rectifying coordinates.

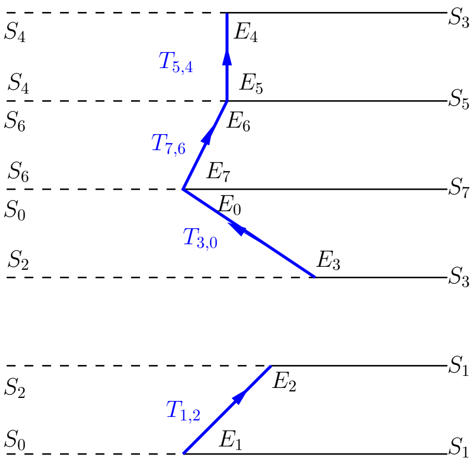

Figure 7: Depiction of the clockwise transversal chains (oriented line segments) $T_{\{[3]\}}$ and $T_{\{[1]\}}$ in rectifying coordinates for the combinatorial invariant depicted in Figure 6.

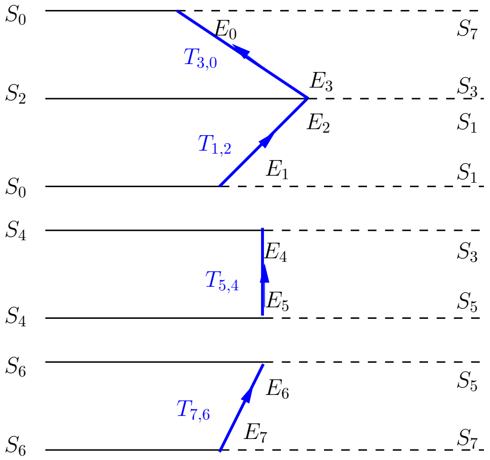

Figure 8: Depiction of the counter-clockwise transversal chains (oriented line segments) $T_{\{[0]\}}$, $T_{\{[4]\}}$, and $T_{\{[6]\}}$ in rectifying coordinates for the combinatorial invariant depicted in Figure 6.

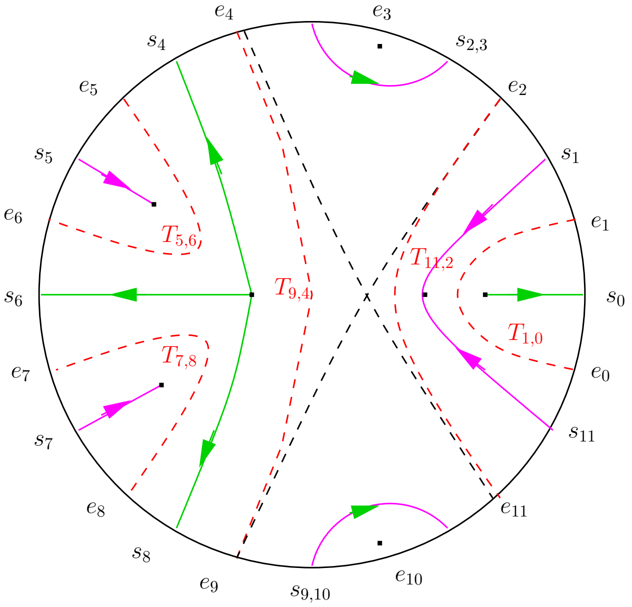

Figure 9: Example of a disk representation of a $\xi_P \in \Xi_7$ that contains two counter-clockwise closed T_P-chains $T_{\{[0]\}}$ and $T_{\{[4]\}}$; three clockwise closed T_P-chains $T_{\{[1]\}}$, $T_{\{[5]\}}$, and $T_{\{[7]\}}$; one counter-clockwise open H_P-chain $H_{\{[9]\}}$; and one clockwise open H_P-chain $H_{\{[2]\}}$. The essential transversals are the grey dashed curves and the non-essential transversals are the black dashed curves.

any equivalence relation $\sim$ on $\mathbb{Z}/(2d-2)$ and any equivalence class $[\ell]$, we let $[\ell]_{\overline{\mathbb{D}}}$ denote the convex hull of the equivalence class $[\ell]$ in the Poincaré metric in $\overline{\mathbb{D}}$, i.e. the smallest convex closed subset of $\overline{\mathbb{D}}$ containing the geodesics joining $\delta_{\ell'}$ and $\delta_{\ell''}$ for any $\ell', \ell'' \in [\ell]$ (see Figure 10).

In light of this representation in the disk, we give the following alternative definition of a non-crossing equivalence relation (compare with Definition 3.7).

Definition 3.14 (Non-crossing equivalence relation)**.** An equivalence relation $\sim$ on $\mathbb{Z}/(2d-2)$ is called *non-crossing* if and only if for any pair of distinct equivalence classes $[\ell_1]$ and $[\ell_2]$, the corresponding convex hulls $[\ell_1]_{\overline{\mathbb{D}}}$ and $[\ell_2]_{\overline{\mathbb{D}}}$ are disjoint.

Definition 3.15 (The disk model associated to $\sim$)**.** Let $\sim$ be any non-crossing equivalence relation on $\mathbb{Z}/(2d-2)$. The connected components of

$$\overline{\mathbb{D}} \setminus \bigcup_{\ell \in \mathbb{Z}/(2d-2)} [\ell]_{\overline{\mathbb{D}}} \tag{24}$$

are called *cells*. The boundary in $\overline{\mathbb{D}}$ of a cell consists of some geodesics connecting $\delta_{\ell'}$ and $\delta_{\ell''}$ for $\ell' \sim \ell''$, some marked points δ_ℓ, and some arcs in $\mathbb{S}^1$ between marked points. The arc on $\mathbb{S}^1$ between $\delta_{\ell-1}$ and δ_ℓ is denoted ϵ_ℓ and referred to as an end in the disk model for $\sim$. Every end is on the boundary of exactly one cell.

We use a similar convention when drawing the transversals in the disk model. For a transversal $T_{k,j}$, we join the midpoint of the arc ϵ_k to the midpoint of the arc ϵ_j by the geodesic in the Poincaré metric.

Remark 3.16. Note that the convex hulls corresponding to the equivalence class for $\sim_P$ drawn in the same disk as the transversals according to the above convention are also non-crossing.

For a vector field $\xi_P \in \Xi_d$, the cells in the disk model are in one-to-one correspondence with the zones of ξ_P. We formulate this in the following proposition by giving natural names to the cells and characterizing the different types.

Proposition 3.17. *Let $\xi_P \in \Xi_d$ be given and let $(\sim_P, H_P)$ be defined as in definition 3.1 The disk model of $\sim_P$ can have up to five different types of cells called an $\alpha\omega$-*cell*, an odd or even* sepal cell*, and an odd or even* center cell *(see Figure 10). The cells are characterized as follows:*

- *A cell is an $\alpha\omega$-*cell *$\Leftrightarrow$ its boundary in $\overline{\mathbb{D}}$ is associated with one counter-clockwise open H_P-chain $H_{\{[k_{i_1}]\}}$ of length $n^+ \geq 0$ and the corresponding $k_{i_1}-1, \sigma\left(k_{i_{n^+}}\right)+1 \notin H_P$; one clockwise open H_P-chain $H_{\{[j_{i_1}]\}}$ of length $n^- \geq 0$ and the corresponding $j_{i_1}-1, \sigma\left(j_{i_{n^-}}\right)+1 \notin H_P$; the corresponding division points δ_ℓ, $\ell \in H_{\{[k_{i_1}]\}}$, $H_{\{[j_{i_1}]\}}$; $n^+ + 1$ odd ends and $n^- + 1$ even ends; and so that $k_{i_1} - 1 \sim_P \sigma\left(j_{i_{n^-}}\right) + 1$ and $\sigma\left(k_{i_{n^+}}\right) + 1 \sim_P j_{i_1} - 1$.*
- *A cell is an odd or an even* sepal cell *$\Leftrightarrow$ its boundary in $\overline{\mathbb{D}}$ is associated with one counter-clockwise (resp. one clockwise) open H_P-chain $H_{\{[k_{i_1}]\}}$ (resp. $H_{\{[j_{i_1}]\}}$) of length $n \geq 0$ and the corresponding $k_{i_1}-1, \sigma(k_{i_n})+1 \notin H_P$ (resp. $j_{i_1}-1, \sigma(j_{i_n})+1 \notin H_P$), the corresponding marked points δ_ℓ, $\ell \in H_{\{[k_{i_1}]\}}$ (resp. $\ell \in H_{\{[j_{i_1}]\}}$), $n+1$ odd (resp. even) ends, and so that $k_{i_1}-1 \sim_P \sigma(k_{i_n})+1$ (resp. $j_{i_1}-1 \sim_P \sigma(j_{i_n})+1$).*

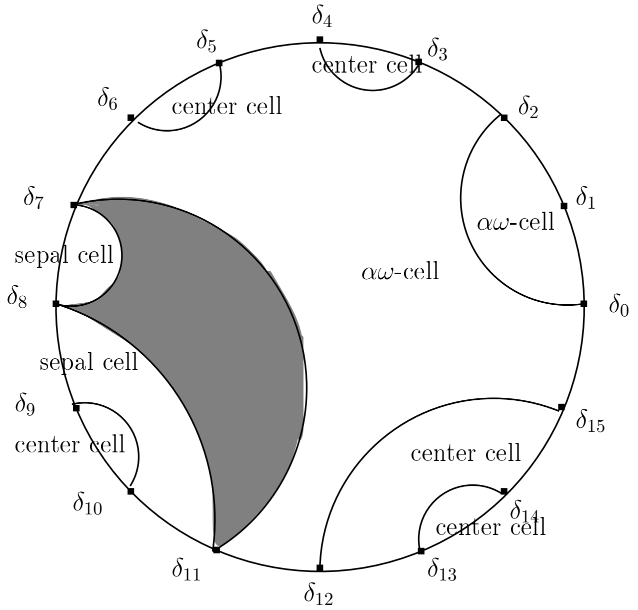

Figure 10: Example of a disk model for $d = 9$ and the different types of cells that can occur for the equivalence classes $H = \{\{3,4\},\{5,6\},\{9,10\},\{12,15\},\{13,14\}\}$, $[0] = \{0,2\}$, $[1] = \{1\}$, and $[7] = \{7,8,11\}$.

- *A cell is an odd or an even* center cell $\Leftrightarrow$ *its boundary in* $\overline{\mathbb{D}}$ *is associated with one counter-clockwise (resp. one clockwise) closed* H_P*-chain* $H_{\{[k_{i_1}]\}}$ *(resp.* $H_{\{[j_{i_1}]\}}$*) of length* $n \geq 1$*, the corresponding marked points* δ_ℓ*,* $\ell \in H_{\{[k_{i_1}]\}}$ *(resp.* $\ell \in H_{\{[j_{i_1}]\}}$*), and the* n *odd (resp. even) ends.*

We now have enough notation in order to give the definition of a combinatorial data set of degree d.

Definition 3.18. A *combinatorial data set* $(\sim, H)$ of degree $d \geq 2$ consists of an equivalence relation $\sim$ on $\mathbb{Z}/\left(2d-2\right)$ and a marked subset $H \subset \mathbb{Z}/\left(2d-2\right)$ satisfying:

1) $\sim$ is non-crossing.

2) If $\ell' \neq \ell''$, then $\ell' \sim \ell''$ and $\ell' \in H \Leftrightarrow \ell'' \in H$ and ℓ' and ℓ'' have different parity.

3) Every cell in the disk-model realization of $(\sim, H)$ is one of the five types: an $\alpha\omega$-cell, an odd or even sepal-cell, or an odd or even center-cell characterized as above.

Let $\mathcal{D}_d$ be the set of combinatiorial data sets of degree d.

Remark 3.19. If $H = \emptyset$ and there are no mixed equivalence classes so that all cells are $\alpha\omega$-cells, then the definition of a combinatorial data set can be formulated equivalently as a non-crossing pairing of even and odd ends. This is the definition used in [DES].

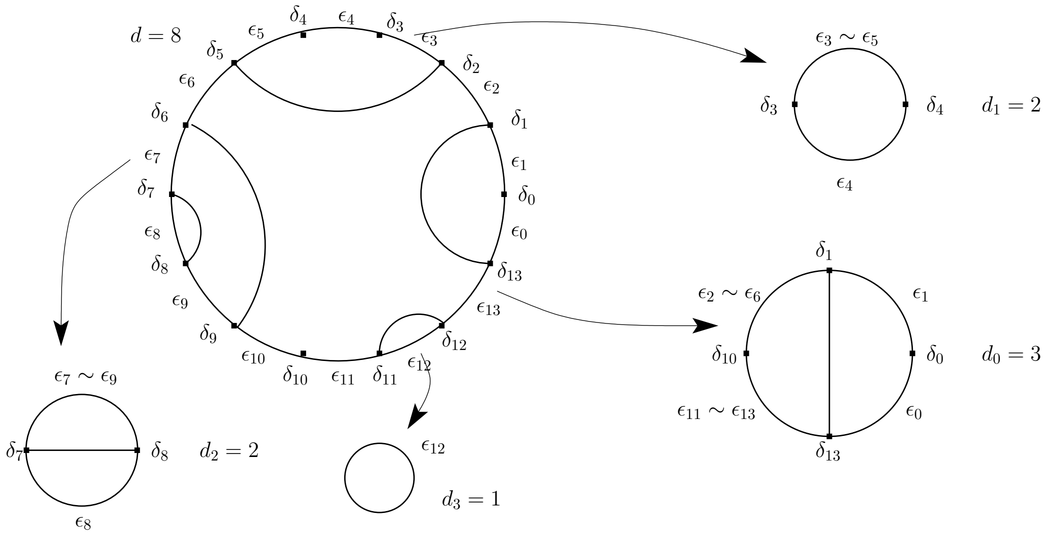

Figure 11: Example of how a disk model can be decomposed by the equivalence classes in $H = \{\{2,5\},\{6,9\},\{11,12\}\}$ to $h+1$ induced disk models where $H = \emptyset$.

Remark 3.20 (Abstractifications)**.** A definition of the different types of cells for $(\sim, H) \in \mathcal{D}_d$ is taken from Proposition 3.17 with $(\sim_P, H_P)$ replaced by $(\sim, H)$. The numbering conventions of the cells for $(\sim, H) \in \mathcal{D}_d$ are likewise analagous to those for zones in 2.1, with the appropriate replacement of terms. The properties of the equivalence classes, H-chains, and T-chains for $(\sim, H) \in \mathcal{D}_d$ are completely analagous to the properties stated for $(\sim_P, H_P)$.

For a given $(\sim, H) \in \mathcal{D}_d$, we let $s = s(\sim, H)$ denote the number of $\alpha\omega$-cells in the disk model of $(\sim, H)$, $p = p(\sim, H)$ denote the number of sepal-cells, $h = h(\sim, H) = \frac{1}{2}|H|$ the number of equivalence classes in H, and $c(\sim, H) = n_c^+ + n_c^-$ the number of closed H-chains.

We analyze the equivalence relation $\sim$ for a given $(\sim, H) \in \mathcal{D}_d$.

Remark 3.21. For $(\sim, H) \in \mathcal{D}_d$, if $H \neq \emptyset$, then $|H|/2 = h$ and $\overline{\mathbb{D}} \setminus \bigcup_{[\ell] \subseteq H} [\ell]_{\overline{\mathbb{D}}}$ consists of $h+1$ connected components. By identifying division points δ_j and δ_k where $\{j,k\} = [k] \subseteq H$ and removing them (and hence identifying the ends ϵ_k with ϵ_{j+1} or ϵ_{k+1} with ϵ_j), we obtain $h+1$ circles $\mathbb{S}_i$, $i = 0, \ldots, h$, each with an even number $2d_i - 2$ (possibly 0) of division points adding up to $2d - 2 - 2h$. Let $L_i = \{\ell \in L \mid \delta_\ell \in \mathbb{S}_i\}$ and $[\ell', \ell'']_{L_i} = [\ell', \ell''] \cap L_i$. Each $\overline{\mathbb{D}}_i$ carries an induced equivalence relation $\sim_i$. A connected component in $\overline{\mathbb{D}} \setminus \bigcup_{[\ell] \subseteq H} [\ell]_{\overline{\mathbb{D}}}$ is a *center cell* if and only if there are no further division points on the boundary of the corresponding $\overline{\mathbb{D}}_i$, i.e. $d_i = 1$, where the $[\ell] \subseteq H$ on the boundary of the component form a closed H-chain. The remaining circles satisfy the following properties outlined in Propositions 3.22 and 3.23 for a combinatorial data set without homoclinic separatrices (see Figure 11).

Proposition 3.22. *Suppose $(\sim, H) \in \mathcal{D}_d$ with $H = \emptyset$. The equivalence relation*

$\sim$ on $L = \mathbb{Z}/\left(2d-2\right)$ has

$$q = d - \frac{1}{2}\sum_{[\ell]\subseteq L} p_{[\ell]} \tag{25}$$

equivalence classes.

Proof. There are two possible types of zones: $\alpha\omega$-zones with two ends, and sepal zones with one end each. By comparing the number of ends, we get the relation

$$2\left(d-1\right) = 2s\left(\sim, H\right) + p\left(\sim, H\right). \tag{26}$$

Note that if $s\left(\sim, H\right) = 0$, then $\sim$ necessarily has only one equivalence class. Assume that $\sim$ has more than one equivalence class, so that $s\left(\sim, H\right) > 0$. The transversals in the $\alpha\omega$-cells divide $\overline{\mathbb{D}}$ into $s\left(\sim, H\right)+1$ subsets, corresponding to the $s\left(\sim, H\right)+1$ equivalence classes. One can see this by noting each subset must correspond to at least one equivalence class since there will be at least one division point on the boundary of the subset, and there cannot be more than one equivalence class, since then there would exist a cell with more than two ends on the boundary. Therefore, $\sim$ has

$$q = s\left(\sim, H\right) + 1 = d - \frac{1}{2}\sum_{[\ell]\subseteq L} p_{[\ell]}, \tag{27}$$

equivalence classes since $p\left(\sim, H\right) = \sum\limits_{[\ell]\subseteq L} p_{[\ell]}$. □

Proposition 3.23. *Suppose $\left(\sim, H\right) \in \mathcal{D}_d$ with $H = \emptyset$, and $\sim$ has more than one equivalence class. For each $\alpha\omega$-cell, the associated transversal $T_{k,j}$ divides the disk model into two connected components U_k and U_j, numbered so that $\delta_i \in \partial U_i$, $i = k, j$. Correspondingly, $L = \mathbb{Z}/\left(2d-2\right)$ is divided into two disjoint subsets I_k and I_j where $\ell \in I_i \Leftrightarrow \delta_\ell \in \partial U_i$. Define d_i by $|I_i| = (2d_i - 2) + 1$, since $|I_i|$ is odd. Then the number of equivalence classes in I_i is*

$$q_i = d_i - \frac{1}{2}\sum_{[\ell]\subseteq I_i} p_{[\ell]}, \quad i = k, j. \tag{28}$$

Proof. Since we assumed $\sim$ has more than one equivalence class, there is always at least one $\alpha\omega$-cell. Choose an $\alpha\omega$-cell, say the one with transversal $T_{k,j}$. It follows that $k \sim j-1$ and $j \sim k-1$. Since $\sim$ is non-crossing, $\sim$ induces an equivalence relation $\sim_k$ on $I_k = [k, j-1]$ and $\sim_j$ on $I_j = [j, k-1]$ by

$$\begin{cases} \ell', \ell'' \in I_k & : \ell' \sim_k \ell'' \\ \ell', \ell'' \in I_j & : \ell' \sim_j \ell'' \end{cases} \Leftrightarrow \ell' \sim \ell''. \tag{29}$$

We think of δ_k as being identified with δ_{j-1} in I_k, and we think of δ_j as being identified with δ_{k-1} in I_j. In the induced circles $\mathbb{S}_k$ and $\mathbb{S}_j$, the number of ends is even: $j-1-k \pmod{2d-2}$ in $\mathbb{S}_k$ and $k-1-j \pmod{2d-2}$ in $\mathbb{S}_j$.

By comparing the number of ends, we must have

$$\begin{aligned} j-1-k &\pmod{2d-2} = 2\left({}_k s\left(\sim, H\right)\right) + {}_k p\left(\sim, H\right) \\ k-1-j &\pmod{2d-2} = 2\left({}_j s\left(\sim, H\right)\right) + {}_j p\left(\sim, H\right), \end{aligned} \tag{30}$$

where ${}_i s\,(\sim, H)$ and ${}_i p\,(\sim, H)$, are the number of $\alpha\omega$-cells and sepal cells for I_i respectively, $i = k, j$. The number of equivalence classes for I_i is $q_i = {}_i s\,(\sim, H)+1$, $i = k, j$. From these relations, one can deduce that the equivalence relation on I_i induces

$$q_i = d_i - \frac{1}{2} \sum_{[\ell] \subseteq I_i} p_{[\ell]} \tag{31}$$

equivalence classes. □

Below are presented some properties of equivalence relations and marked subsets H satisfying 1) and 2) in Definition 3.18. These *decomposition properties* will prove to be equivalent with 3) in Definition 3.18.

Definition 3.24 (Decomposition Properties)**.** Let $\sim$ be an equivalence relation on $\mathbb{Z}/\left(2d-2\right)$ and $H \subseteq \mathbb{Z}/\left(2d-2\right)$ a marked subset satisfying 1) and 2) in Definition 3.18. The equivalence relation $\sim$ together with H is said to satisfy the *decomposition properties* if the following conditions hold.

i. Let $h = |H|/2$ (possibly 0). Then in each of the $h+1$ connected components $\overline{\mathbb{D}}_i$ of $\overline{\mathbb{D}} \setminus \bigcup_{[\ell] \subseteq H} [\ell]_{\overline{\mathbb{D}}}$ in the disk model, where we define d_i by setting $2d_i - 2$ equal to the number of division points, there are exactly

$$d_i - \frac{1}{2} \sum_{[\ell] \subseteq L_i} p_{[\ell]}, \quad i = 0, \ldots, h \tag{32}$$

equivalence classes in that component if $d_i > 1$, and no equivalence classes in a component where $d_i = 1$.

ii. For every partition $I_0 = [\ell_0, \ell_1]$ and $I_1 = [\ell_1 + 1, \ell_0 - 1]$ of the equivalence classes of $\sim$ with $|I_0|$ and $|I_1|$ odd (i.e. ℓ_0 and ℓ_1 of the same parity), then I_0 has

$$\frac{\ell_1 - \ell_0 + 2}{2} - \frac{1}{2} \sum_{[\ell] \subseteq I_0} p_{[\ell]} \tag{33}$$

equivalence classes and I_1 has

$$\frac{2d - 2 + \ell_0 - \ell_1}{2} - \frac{1}{2} \sum_{[\ell] \subseteq I_1} p_{[\ell]} \tag{34}$$

equivalence classes.

iii. For every $\ell \in L_i$, $\sigma\left(\ell\right) - \ell$ is either even or $[\ell + 1, \sigma\left(\ell\right) - 1]_{L_i} = \emptyset$.

We now show the above properties are equivalent with 3) in Definition 3.18, given 1) and 2).

Theorem 3.25 (Characterization of a combinatorial data set $(\sim, H) \in \mathcal{D}_d$)**.** *Let $\sim$ be an equivalence relation and a marked set $H \subseteq \mathbb{Z}/\left(2d-2\right)$ satisfying* 1) *and* 2) *in Definition 3.18. Then $(\sim, H)$ satisfies* 3) *in Definition 3.18 if and only if $(\sim, H)$ has the decomposition properties in Definition 3.24.*

We first need a definition and several lemmas to prove this.

Lemma 3.26.

1. *Given an equivalence relation $\sim$ on $\mathbb{Z}/(2d-2)$, $d > 2$ with $H = \emptyset$ satisfying property 1) in Definition 3.18 and the decomposition properties, there exists some distinct $\ell' \sim \ell''$ of the same parity.*

2. *For $I = [\ell+1, \sigma(\ell)-1]$, if $\sigma(\ell) - \ell > 2$, then there exists some $\ell' \sim \ell'' \in I$ of the same parity.*

Proof by contradiction. Assume not. Then an equivalence class can contain at most 2 elements: one even and one odd. Let n be the number of elements in equivalence classes by themselves.

1. Note that n must necessarily be even. Then the number of equivalence classes is $n + \frac{2(d-1)-n}{2}$. Now by the first counting property, the number of equivalence classes should be equal to $d - \frac{1}{2}\sum\limits_{[\ell]\subseteq L} p_{[\ell]} = d - \left(\frac{2(d-1)-n}{2}\right) = \frac{2+n}{2}$, which implies that $d = 2$.

2. Note that n must necessarily be odd. Let $2s+1 = \sigma(\ell) - \ell - 1 = |I|$. The number of equivalence classes is $n + \frac{2s+1-n}{2}$. By the second decomposition property, the number of equivalence classes should be equal to $s + 1 - \frac{1}{2}\sum\limits_{[\ell]\subseteq I} p_{[\ell]} = \frac{1+n}{2}$. This implies that $s = 0$ and $\sigma(\ell) - \ell = 2$.

□

Lemma 3.27. *Given an equivalence relation $\sim$ on $\mathbb{Z}/(2d-2)$, $d > 2$, with $H = \emptyset$ satisfying property 1) in Definition 3.18 and the decomposition properties, there exists some ℓ such that $\ell \sim \ell + 2$.*

Proof. By Lemma 3.26, there exists some $\ell, \sigma(\ell)$ of the same parity with $\sigma(\ell) \geq \ell + 2$. If $\sigma(\ell) = \ell + 2$, then we are finished. If $\sigma(\ell) \geq \ell + 4$, then we consider the integers $I = [\ell + 1, \sigma(\ell) - 1]$. Since I is disjoint from $[\sigma(\ell), \ell]$, we can use the second decomposition property to conclude that they cannot all be in equivalence classes by themselves. If all $\ell \in I$ are in the same equivalence class then we are again finished. If they are not all in the same equivalence class, then we can use Lemma 3.26 (2) to conclude that there must again exist $\ell' \sim \sigma(\ell') \in I$ of the same parity with $\sigma(\ell') - \ell' \leq \sigma(\ell) - \ell - 2$. Repeating this process forms nested subsets of integers, whose maximum difference is strictly decreasing and always even. Since these are never empty, we must have the claim fulfilled. □

Definition 3.28. Given a non-crossing equivalence relation $\sim$ on $\mathbb{Z}/(2d-2)$, $d > 2$, the *basic partition with basepoint* ℓ_0 is the set of consecutive closed intervals

$$\underbrace{[\ell_0, \ell_1]}_{I_0} \quad \underbrace{[\ell_1 + 1, \ell_2]}_{I_1} \quad \ldots \quad \underbrace{[\ell_{n-1} + 1, \ell_n = \ell_0 + 2d - 3]}_{I_{n-1}} \tag{35}$$

such that

$$\begin{aligned} \ell_0 \sim \ell_1, \quad \ell_1 \nsim \ell \in \sum_{i=1}^{n-1} I_i \\ \ell_1 + 1 \sim \ell_2, \quad \ell_2 \nsim \ell \in \sum_{i=2}^{n-1} I_i \\ \vdots \qquad\qquad \\ \ell_{n-1} + 1 \sim \ell_n = \ell_0 + 2d - 3. \end{aligned}$$

Lemma 3.29. *Given an equivalence relation $\sim$ on $\mathbb{Z}/(2d-2)$, $d > 2$, with $H = \emptyset$ satisfying property 1) in Definition 3.18 and the decomposition properties, then for any ℓ_0, the basic partition with basepoint ℓ_0 consists of exactly two intervals if $\ell_0 \nsim \ell_0 + 2d - 3$ and one interval if $\ell_0 \sim \ell_0 + 2d - 3$.*

Proof. If $\ell_0 \sim (\ell_0 + 2d - 3)$, then $I_0 = [\ell_0, \ell_0 + 2d - 3]$. Suppose $\ell_0 \nsim (\ell_0 + 2d - 3)$ and let $I_0, \ldots, I_{n-1}$ be the basic partition with basepoint ℓ_0. Note that $\ell_i + 1 \sim \ell_{i+1}$, $i = 0, \ldots, n-1$, have the same parity by the third decomposition property, and $n \geq 2$. If each I_i, $i = 0, \ldots, n-1$ gives rise to q_i equivalence classes, each having a total number of parity changes

$$\sum_{[\ell] \subseteq I_i} p_{[\ell]}, \tag{36}$$

then we must have the relation

$$d - \sum_{i=0}^{k-1} q_i = \sum_{i=0}^{k-1} \frac{1}{2} \sum_{[\ell] \subseteq I_i} p_{[\ell]}. \tag{37}$$

We set

$$d_i := \frac{\ell_i - \ell_{i-1} + 1}{2}, \quad i = 0, \ldots, n-1. \tag{38}$$

Now each I_i must satisfy the decomposition properties, so we further have the relation

$$d_i - q_i = \frac{1}{2} \sum_{[\ell] \subseteq I_i} p_{[\ell]}, \tag{39}$$

and Equation (38) gives

$$2 \sum_{i=0}^{n-1} d_i = n + \ell_n + 1 = 2d - 2 + n. \tag{40}$$

Now (39) and (37) gives

$$\sum_{i=0}^{k-1} d_i = d, \tag{41}$$

so

$$2d = 2d - 2 + n, \tag{42}$$

which implies that $n = 2$. □

Lemma 3.30. *Given an equivalence relation* $\sim$ *on* $\mathbb{Z}/(2d-2)$, $d > 2$, *with* $H = \emptyset$ *satisfying property 1) in Definition 3.18 and the decomposition properties, if* $[\ell] \subseteq [\ell_0, \ell_1]$ *and* $\ell_0,\ \ell_1 \in [\ell]$, *then* $\ell_0 - 1 \sim \ell_1 + 1$.

Proof. If $\ell_1 = \ell_0 + 2d - 3$, this is trivially true. If $\ell_1 \neq \ell_0 + 2d - 3$, then ℓ_0 and ℓ_1 have the same parity and $I_0 = [\ell_0, \ell_1]$ together with $I_1 = [\ell_1 + 1, \ell_0 + 2d - 3]$ must be the basic partition with basepoint ℓ_0. Hence, $\ell_1 \sim \ell_0 + 2d - 3 = \ell_0 - 1 \,(\mod 2d - 2)$. □

We are now ready to prove the theorem.

Proof of Theorem 3.25. We first show that for $(\sim, H) \in \mathcal{D}_d$, the decomposition properties hold.

Remark 3.21 and Proposition 3.22 imply property *i.*, and the fact that a sepal cell has only one end on its boundary when $H = \emptyset$ implies property *iii.*. Proposition 3.23 proves property *ii.* and finishes the first half of the proof.

We now prove that if $\sim$ and H satisfy 1) and 2) from Definition 3.18 and the decomposition properties, then $(\sim, H) \in \mathcal{D}_d$ (i.e. 3) from 3.18 holds). That is, we need to prove that we can only have cells of the types specified in 3). If $H \neq \emptyset$, then the disk model is decomposed into $h + 1$ components $\overline{\mathbb{D}}_i$ with associated d_i, $i = 0, \ldots, h$. If $d_i = 1$, then the $[\ell] \subseteq H$ on $\partial\overline{\mathbb{D}}_i$ must necessarily form a closed H-chain, corresponding to a center cell (see Remark 3.21). It is otherwise enough to consider the case $H = \emptyset$. An $\alpha\omega$-cell exists when there is one even end ϵ_j and one odd end ϵ_k on its boundary. A sepal-cell exists when there is exactly one end on its boundary. We prove 3) by induction on d. It is true for $d = 2$. Indeed, for $d = 2$, we have for $H = \emptyset$ either $[0] = \{0\}$ and $[1] = \{1\}$ or $[0] = \{0, 1\}$. In the first case, ϵ_0 and ϵ_1 are the only ends on the boundary of the same cell (i.e. an $\alpha\omega$-cell). In the second case, ϵ_0 and ϵ_1 are each the only end on the boundary of different cells (i.e. sepal cells). Assume now that there are only $\alpha\omega$-cells with one odd and one even end on the boundary and sepal cells with one end on the boundary for all d. Then for $d + 1$, we have that some equivalence class either contains only one element or there is an equivalence class having at least three consecutive elements by Lemma 3.27. If the first case, we can assume without loss of generality that $[0] = \{0\}$. Then we know by Corollary 3.30 that $1 \sim 2d - 3$ and hence ϵ_0 and ϵ_1 are on the boundary of an $\alpha\omega$-cell. If we identify δ_1 and δ_{2d-3} and remove δ_0, then we have a degree d equivalence relation, whose induced equivalence relation on the ends has only $\alpha\omega$-cells and sepal cells by assumption. Hence, we again only have cells of the desired types.

If the second case, then we can assume without loss of generality that $(2d - 3) \sim 0 \sim 1$. Then the ends ϵ_0 and ϵ_1 are each on the boundary of a sepal cell. Again, we can identify δ_1 and δ_{2d-3} and remove δ_0, then we have a degree d equivalence relation, whose induced equivalence relation on the ends has only $\alpha\omega$-cells and sepal cells by assumption. Hence, there must be only cells of the desired type for all $d \geq 2$. □

4 Analytic Invariants

We have defined a combinatorial invariant describing the topological properties of any $\xi_P \in \Xi_d$. Our aim is to define a set of analytic invariants describing the geometric properties.

It seems natural to consider the *dynamical residues* (defined below) of the equilibrium points as analytic invariants, as these determine the local normal form of the vector field in a neighborhood of each equilibrium point (see for instance [BT76]), but we will see that there is in fact a better choice (see Definition 4.4).

Definition 4.1 (Dynamical residues of ξ_P)**.** Let ζ be an arbitrary equilibrium point of ξ_P, i.e. a root of P. Let γ be a simple, closed, oriented curve not intersecting any equilibrium points and winding counter-clockwise around exactly one equilibrium point ζ. Then the *dynamical residue* of ξ_P at ζ is defined as

$$\rho(\zeta) = \int_\gamma \frac{dz}{P(z)} = 2\pi i \operatorname{Res}\left(\frac{1}{P}, \zeta\right). \tag{43}$$

Remark 4.2. Applying the usual formula for residues, we have

$$\rho(\zeta) = 2\pi i \lim_{z\to\zeta} \frac{1}{(m-1)!} \frac{d^{m-1}}{dz^{m-1}} \left[(z-\zeta)^m \frac{1}{P(z)} \right] \tag{44}$$

if ζ is a multiple root of multiplicity m. In particular, if ζ is a simple root, then

$$\rho(\zeta) = \frac{2\pi i}{P'(\zeta)}. \tag{45}$$

Note that we could allow the above curve γ to be the piecewise smooth (closed, but not simple) curve consisting of T_P-chains and H_P-chains bounding the equilibrium point and the separatrices it receives, together with the point at infinity (see Figure 12). More specifically,

- For a center, we let γ be the counter-clockwise (or clockwise) H_P-chain on the boundary of its zone, together with $\{\infty\}$.
- For a multiple equilibrium point $\zeta_{[m]}$, we let

$$\gamma = \{\infty\} \cup \bigcup_{\sigma(j)-j \text{ odd}} H_{\{[j+1]\}} \cup \bigcup_{\sigma(k)-k \text{ odd}} H_{\{[k+1]\}} \cup \bigcup_{\sigma(\ell)-\ell \text{ even}} T_{\{[\ell+1]\}}, \tag{46}$$

  for $j,\ k,\ \ell \in [m]$.
- For a source or sink $\zeta_{[\ell]}$, we let

$$\gamma = \{\infty\} \cup T_{\{[\ell+1]\}}. \tag{47}$$

The point at infinity does not cause any problems. The singularity for $\frac{dz}{P(z)}$ at ∞ is for $d \geq 2$ a removable singularity, in particular a zero for $d > 2$. Indeed,

$$\left(\frac{-1}{z^2}\right)\left(\frac{1}{P\left(\frac{1}{z}\right)}\right) = \frac{-z^{d-2}}{1 + a_{d-2}z^2 + \cdots + a_0 z^d}. \tag{48}$$

Remark 4.3. Since the dynamical residues are simply sums of the integrals of $\frac{dz}{P(z)}$ over transversals and homoclinic separatrices, it makes sense for these to be the analytic invariants instead. However, if we considered integrals over all

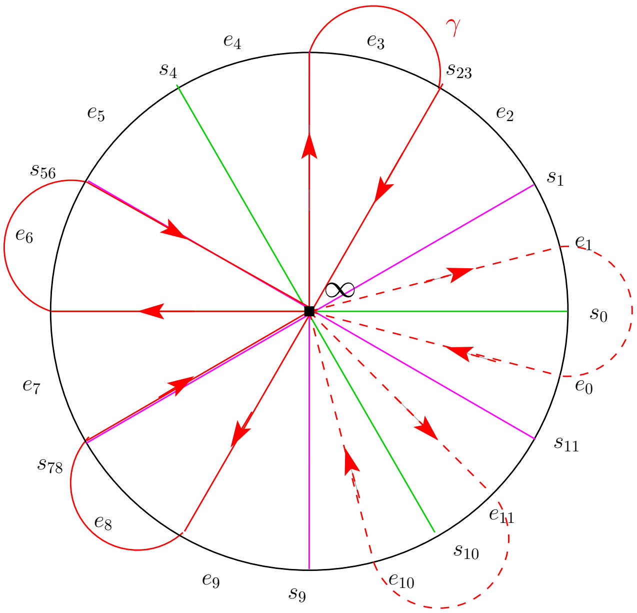

Figure 12: Depiction of how γ might be made from a union of homoclinic separatrices (solid oriented curves) and transversals (dashed oriented curves). Compare with Figure 5.

transversals, these would contain superfluous information if at least one of the $\alpha\omega$-zones has a homoclinic separatrix on the boundary, since any integral over a transversal is a sum of the integral over some other transversal and integrals over appropriate homoclinic separatrices. Therefore, for each $\alpha\omega$-zone, the integral over only one transversal is needed to retain the same information.

We therefore choose a convention after the numbering of the zones (see Subsection 2.1) and state the definition.

Definition 4.4 (Definition of analytic invariants of ξ_P)**.** Let $\xi_P \in \Xi_d$ be given.

1. The *analytic invariant* of an $\alpha\omega$-zone $Z_{k,j}^{\alpha\omega}$ of ξ_P is defined as

$$\alpha\left(Z_{k,j}^{\alpha\omega}\right) = \int_{e_k}^{e_j} \frac{dz}{P\left(z\right)}, \tag{49}$$

   where the integral is along any curve γ_Z in $Z_{k,j}^{\alpha\omega}$ connecting e_k to e_j (see Figure 13).

2. The *analytic invariant* of a homoclinic separatrix $s_{k,\sigma(k)}$ of ξ_P is defined as

$$\tau\left(s_{k,\sigma(k)}\right) = \int_{s_{k,\sigma(k)}} \frac{dz}{P\left(z\right)}. \tag{50}$$

3. The *total analytic invariant* of ξ_P is

$$A\left(\xi_P\right) = \left(\alpha_1\left(\xi_P\right), \ldots, \alpha_{s_P}\left(\xi_P\right), \tau_1\left(\xi_P\right), \ldots, \tau_{h_P}\left(\xi_P\right)\right), \tag{51}$$

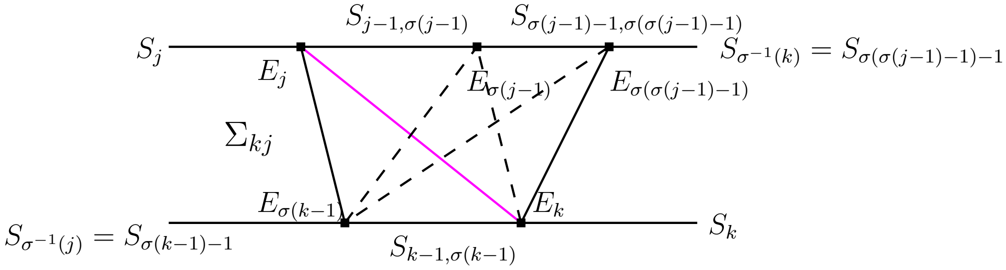
$S_{j-1,\sigma(j-1)}$
$S_{\sigma(j-1)-1,\sigma(\sigma(j-1)-1)}$
S_j
$S_{\sigma^{-1}(k)} = S_{\sigma(\sigma(j-1)-1)-1}$
E_j
$E_{\sigma(j-1)}$
$E_{\sigma(\sigma(j-1)-1)}$
Σ_{kj}
$E_{\sigma(k-1)}$
E_k
$S_{\sigma^{-1}(j)} = S_{\sigma(k-1)-1}$
S_k
$S_{k-1,\sigma(k-1)}$

Figure 13: The strip $\Sigma_{k,j}$ associated to an $\alpha\omega$-zone $Z^{\alpha\omega}_{k,j}$. The transversals are drawn in the strip where the solid black lines are the essential transversals, the solid grey line is the transversal defining the analytic invariant associated to $Z^{\alpha\omega}_{k,j}$, and the dashed lines are some other non-essential transversals.

where $\alpha_i(\xi_P) = \alpha\left(Z^{\alpha\omega}_{k_i,j_i}\right)$, $i = 1, \ldots, s_P$, and $\tau_i(\xi_P) = \tau\left(s_{k_i,\sigma(k_i)}\right)$, $i = 1, \ldots, h_P$.

Proposition 4.5 (from [DES]). *Let $\xi_P \in \Xi_d$ be given.*

1. *For any $\alpha\omega$-zone Z of ξ_P, the invariant $\alpha(Z)$ belongs to $\mathbb{H}$ and $\Im(\alpha(Z))$ is equal to the height of the horizontal strip described in Theorem 2.16.*
2. *For any homoclinic separatrix s of ξ_P, the invariant $\tau(s)$ belongs to $\mathbb{R}_+$.*

Remark 4.6.

1. It follows from Proposition 4.5 that $A(\xi_P) \in \mathbb{H}^{s_P} \times \mathbb{R}_+^{h_P}$.
2. We may refer to the invariant $\alpha\left(Z^{\alpha\omega}_{k,j}\right)$ as the complex "time" it takes to go from the end e_k to the end e_j in the $\alpha\omega$-zone $Z^{\alpha\omega}_{k,j}$ (see [DES] or [BT07] for elaboration).
3. The invariant $\tau\left(s_{k,\sigma(k)}\right)$ is the (real) time it takes to go along the homoclinic separatrix $s_{k,\sigma(k)}$ from ∞ to ∞ in the direction given by k to $\sigma(k)$.

Later, we will be interested in the sum of all analytic invariants associated to an H_P-chain. Therefore, we now define

$$\tau_{\{[k_{i_1}]\}}(\xi_P) = \sum_{\nu=1}^{n} \tau_{i_\nu}(\xi_P), \tag{52}$$

corresponding to the counter-clockwise H_P-chain $H_{\{[k_{i_1}]\}}$ of length n and

$$\tau_{\{[j_{i_1}]\}}(\xi_P) = \sum_{\nu=1}^{n} \tau_{i_\nu}(\xi_P), \tag{53}$$

corresponding to the clockwise H_P-chain $H_{\{[j_{i_1}]\}}$ of length n.

We will also often be interested in the integral of $\frac{dz}{P(z)}$ over an essential transversal which is a linear combination of the analytic invariants associated to a strip. For a strip $\Sigma_{k,j}$, the complex time associated to the essential transversals $T_{\sigma^{-1}(j)+1,j}$ and $T_{k,\sigma^{-1}(k)+1}$ is defined as

$$\alpha_i^-(j) = \alpha_i + \tau_{\{[\sigma^{-1}(j)+1]\}} \quad \text{and} \tag{54}$$

$$\alpha_i^+(k) = \alpha_i + \tau_{\{[\sigma^{-1}(k)+1]\}} \tag{55}$$

respectively.

Applying the Residue Theorem, we obtain the following relations between the analytic invariants and the dynamical residues.

1. For an $\alpha\omega$-zone $Z_{k,j}^{\alpha\omega}$ and for any curve γ_Z in $Z_{k,j}^{\alpha\omega}$ connecting e_k to e_j,

$$\alpha\left(Z_{k,j}^{\alpha\omega}\right) = \sum_{\zeta \text{ left of } \gamma_Z} \rho(\zeta). \tag{56}$$

2. For a homoclinic separatrix s:

$$\tau(s) = \sum_{\zeta \text{ left of } s} \rho(\zeta). \tag{57}$$

3. For a source $\zeta_{[j]}$:

$$\rho\left(\zeta_{[j]}\right) = \sum_{j' \in [j]} \alpha_i^-(j'). \tag{58}$$

4. For a sink $\zeta_{[k]}$:

$$\rho\left(\zeta_{[k]}\right) = \sum_{k' \in [k]} \alpha_i^+(k') \tag{59}$$

(see Remark 4.3 and Figure 13).

5. For a center ζ:

$$\rho(\zeta) = \pm \sum_{s \subset \partial \mathcal{B}(\zeta)} \tau(s) \tag{60}$$

with "+" if $\Im(P'(\zeta)) > 0$ and "−" if $\Im(P'(\zeta)) < 0$ and where we sum over all homoclinic separatrices on the boundary of $\mathcal{B}(\zeta)$, the basin of the center.

If there are q equilibrium points which are not centers, having muliplicities m_i, $i = 1, \ldots, q$, then s_P and h_P satisfy

$$s_P + h_P = d - 1 - \frac{p_P}{2}. \tag{61}$$

The number of equilibrium points including centers but not counting multiplicity $|P^{-1}(0)| = d - \frac{p_P}{2}$ is equal to the number of dynamical residues, so we can conclude from Equation (61) that the number of analytic invariants $s + h$ is always one less than the number of dynamical residues. The superfluous information in one of these dynamical residues is due to the fact that by centering, the position of one of the roots is completely determined by the positions of the others.

Remark 4.7 (Abstractifications)**.** The abstractifications of dynamical residue and analytic invariant and the respective numbering of these for $(\sim, H) \in \mathcal{D}_d$ are analagous to the definitions given for $\xi_P \in \Xi_d$, by replacing $\alpha_i(\xi_P)$ with $\alpha_i(\sim, H)$, $\tau_i(\xi_P)$ with $\tau_i(\sim, H)$, H_P and T_P-chains with H and T-chains, and $\rho\left(\zeta_{[\ell]}\right)$ with $\rho_{[\ell]}$.

The analytic data sets associated to $(\sim, H)$ are all $(s+h)$-tuples in $\mathbb{H}^s \times \mathbb{R}_+^h$, i.e.

$$\mathcal{A}(\sim, H) = \mathbb{H}^s \times \mathbb{R}_+^h. \tag{62}$$

Definition 4.8. For any $(\sim, H) \in \mathcal{D}_d$ and any $A \in \mathcal{A}(\sim, H)$, we say that $\xi_P \in \Xi_d$ *realizes* $(\sim, H)$ and A if and only if $(\sim_P, H_P) = (\sim, H)$ (hence $s_P = s$ and $h_P = h$) and $A(\xi_P) = A$.

5 Equivalence of Flows within a Combinatorial Class

To every polynomial vector field $\xi_P \in \Xi_d$, we associate a combinatorial invariant and analytic invariants. This section will show that vector fields within a combinatorial class have equivalent flows, and that a fixed analytic invariant within this class can only correspond to one vector field.

Let $P_1,\ P_2 \in \mathcal{P}_d$. For simplicity, we use for $i = 1, 2$ the notation $\xi_{P_i} = \xi_i$, $\sim_{P_i} = \sim_i$, $H_{P_i} = H_i$, $s_{P_i} = s_i$, $h_{P_i} = h_i$, etc.

Theorem 5.1. *The vector fields associated with two polynomials P_1 and P_2 having the same combinatorial data set, i.e. $(\sim_1, H_1) = (\sim_2, H_2)$, have quasi-conformally equivalent flows.*

Proof. We will in several steps construct a quasi-conformal homeomorphism $\psi : \mathbb{C} \to \mathbb{C}$ that makes the flows of ξ_1 and ξ_2 equivalent. In particular, equilibrium points of ξ_1 are mapped to equilibrium points of ξ_2 and separatrices to separatrices, but the parameterization by time is not necessarily preserved but is always piecewise linear (to be shown). The mapping ψ is constructed such that the numbering of the separatrices is preserved, in particular $\psi(s_0(\xi_1)) = s_0(\xi_2)$.

Since $(\sim_1, H_1) = (\sim_2, H_2)$, we have the same equivalence classes in $H := H_1 = H_2$ and $\sim := \sim_1 = \sim_2$, the same number of zones of the different types, and the same open and closed H-chains. We will construct

$$\psi : \mathbb{C} \setminus (\Gamma_1 \cup \overline{\gamma}_e(\xi_1)) \to \mathbb{C} \setminus (\Gamma_2 \cup \overline{\gamma}_e(\xi_2)), \tag{63}$$

where the $\overline{\gamma}_e(\xi_i)$ are the curves removed from the center zones for ξ_i as described in Remark 2.17 together with the corresponding center. The isomorphism ψ is constructed by mapping zones of ξ_1 to zones of ξ_2, respecting the different types and numbering as follows.

For any $\nu = 1, \ldots, n_c^+$, let

$$\psi : \left(Z_{k_\nu}^c(\xi_1) \setminus \overline{\gamma}_{e_{k_\nu}}(\xi_1)\right) \to \left(Z_{k_\nu}^c(\xi_2) \setminus \overline{\gamma}_{e_{k_\nu}}(\xi_2)\right) \tag{64}$$

be equal to $\phi_2^{-1} \circ A \circ \phi_1$ where ϕ_1 and ϕ_2 are the rectifying coordinates from Proposition 2.16 mapping the sliced odd center-zones $\left(Z_{k_\nu}^c(\xi_i) \setminus \overline{\gamma}_{e_{k_\nu}}(\xi_i)\right)$ to the upper vertical half-strips $C_{k_\nu}(\xi_i)$, and let $A : C_{k_\nu}(\xi_1) \to C_{k_\nu}(\xi_2)$ be a piecewise-affine mapping constructed as follows. If the number of homoclinic separatrices on the boundaries of $C_{k_\nu}(\xi_i)$ is n, then for simplicity we renumber the ends on the boundaries of the $C_{k_\nu}(\xi_i)$ from left to right

$$E_{k_\nu} := E_{k_1} = 0 < E_{k_2} < \cdots < E_{k_n} < E_{k_{n+1}} = \tau_{\{[k_\nu]\}}, \tag{65}$$

where $E_{k_{n+1}}$ also represents E_{k_1}. We then decompose both $C_{k_\nu}(\xi_i)$ into n vertical half-strips $C^m_{k_\nu}(\xi_i)$, $m = 1, \ldots, n$, where

$$C^m_{k_\nu}(\xi_i) = \left\{ z \in \mathbb{H} \mid E_{k_m}(\xi_i) \le \Re(z) \le E_{k_{m+1}}(\xi_i) \right\}. \tag{66}$$

We define A_m on each $C^m_{k_\nu}(\xi_1)$ so that

$$\begin{bmatrix} \tau\left(S_{k_m,k_{m+1}-1}(\xi_1)\right) \\ 0 \end{bmatrix} \mapsto \begin{bmatrix} \tau\left(S_{k_m,k_{m+1}-1}(\xi_2)\right) \\ 0 \end{bmatrix} \quad \text{and} \quad \begin{bmatrix} 0 \\ 1 \end{bmatrix} \mapsto \begin{bmatrix} 0 \\ 1 \end{bmatrix}, \tag{67}$$

so that the associated matrix $\underline{A}_m$ becomes

$$\underline{A}_m = \begin{bmatrix} \frac{\tau\left(S_{k_m,k_{m+1}-1}(\xi_2)\right)}{\tau\left(S_{k_m,k_{m+1}-1}(\xi_1)\right)} & 0 \\ 0 & 1 \end{bmatrix}, \tag{68}$$

and

$$A_m(x+iy) = \frac{\tau\left(S_{k_m,k_{m+1}-1}(\xi_2)\right)}{\tau\left(S_{k_m,k_{m+1}-1}(\xi_1)\right)} x + iy + \mathcal{T}_m, \tag{69}$$

where $\mathcal{T}_m$ is the appropriate positive real constant. It is similar for the even center zones.

For any $\nu = 1, \ldots, \frac{1}{2}p(\sim, H)$, let

$$\psi : Z^s_{k_\nu}(\xi_1) \to Z^s_{k_\nu}(\xi_2) \tag{70}$$

be equal to $\phi_2^{-1} \circ A \circ \phi_1$ where ϕ_1 and ϕ_2 are the rectifying coordinates from Proposition 2.16 mapping the odd sepal zones $Z^s_{k_\nu}(\xi_i)$ to the upper half-planes $\mathbb{H}_{k_\nu}(\xi_i)$, and $A : \mathbb{H}_{k_\nu}(\xi_1) \to \mathbb{H}_{k_\nu}(\xi_2)$ is a piecewise-affine mapping constructed as follows. If the number of homoclinic separatrices on the boundaries of $\mathbb{H}_{k_\nu}(\xi_i)$ is n, then for simplicity we renumber the $n+1$ ends on the boundaries of the $\mathbb{H}_{k_\nu}(\xi_i)$ from left to right

$$E_{k_\nu} := E_{k_1} = 0 < E_{k_1} < \cdots < E_{k_n} < E_{k_{n+1}} = \tau_{\{[k_\nu]\}}. \tag{71}$$

We then decompose both $\mathbb{H}_{k_\nu}(\xi_i)$ into $n+2$ subsets $H^m_{k_\nu}(\xi_i)$, $m = 1, \ldots, n$, where

$$H^0_{k_\nu}(\xi_i) = \{ z \in \mathbb{H} \mid -\infty < \Re(z) \le E_{k_1}(\xi_i) \} \tag{72}$$
$$H^m_{k_\nu}(\xi_i) = \left\{ z \in \mathbb{H} \mid E_{k_m}(\xi_i) \le \Re(z) \le E_{k_{m+1}}(\xi_i) \right\} \tag{73}$$
$$H^{n+1}_{k_\nu}(\xi_i) = \left\{ z \in \mathbb{H} \mid E_{k_{n+1}}(\xi_i) \le \Re(z) < \infty \right\}, \tag{74}$$

We define A_m on each $H^m_{k_\nu}(\xi_1)$ to be

$$A(x+iy) = \begin{cases} \text{id} & \text{for } m = 0 \\ A_m(x+iy) \text{ from Equation (69)} & \text{for } m = 1, \ldots, n\,. \\ \text{id} + \tau_{\{[k_\nu]\}}(\xi_2) - \tau_{\{[k_\nu]\}}(\xi_1) & \text{for } m = n+1 \end{cases} \tag{75}$$

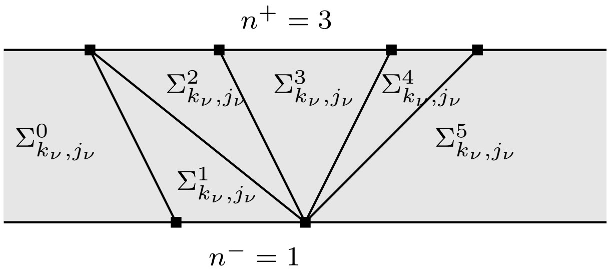

Figure 14: Depiction of a possible decomposition of Σ_{k_ν,j_ν} into $n+2=6$ subsets $\Sigma^m_{k_\nu,j_\nu}$, $m = 0,\ldots,5$. There is one triangle $\Sigma^1_{k_\nu,j_\nu}$ that has an edge contained in the counter-clockwise H-chain on the boundary, and there are three triangles $\Sigma^m_{k_\nu,j_\nu}$, $m = 2,\ldots,4$ having an edge in the clockwise H-chain on the boundary.

It is similar for the even sepal zones.

For any $\nu = 1,\ldots,s(\sim,H)$, let

$$\psi : Z^{\alpha\omega}_{k_\nu,j_\nu}(\xi_1) \to Z^{\alpha\omega}_{k_\nu,j_\nu}(\xi_2) \tag{76}$$

be equal to $\phi_2^{-1} \circ A \circ \phi_1$ where ϕ_1 and ϕ_2 are the rectifying coordinates from Proposition 2.16 mapping the $\alpha\omega$-zones $Z^{\alpha\omega}_{k_\nu,j_\nu}(\xi_i)$ to the horizontal strips $\Sigma_{k_\nu,j_\nu}(\xi_i)$, and $A : \Sigma_{k_\nu,j_\nu}(\xi_1) \to \Sigma_{k_\nu,j_\nu}(\xi_2)$ is a piecewise-affine mapping constructed as follows. If the number of homoclinic separatrices on the upper boundary of the $\Sigma_{k_\nu,j_\nu}(\xi_i)$ is n^- and the number of homoclinic separatrices on the lower boundary of the $\Sigma_{k_\nu,j_\nu}(\xi_i)$ is n^+, then we set $n = n^+ + n^-$ and decompose the $\Sigma_{k_\nu,j_\nu}(\xi_i)$ into $n+2$ subsets $\Sigma^m_{k_\nu,j_\nu}(\xi_i)$, $m = 0,\ldots,n+1$, where $\Sigma^0_{k_\nu,j_\nu}$ is the left most part of the strip bounded by the separatrices S_{j_ν} and $S_{\sigma^{-1}(j_\nu)}$ and the transversal $T_{\sigma^{-1}(j_\nu)+1,j_\nu}$, and $\Sigma^{n+1}_{k_\nu,j_\nu}(\xi_i)$ is the right most part of the strip bounded by the separatrices S_{k_ν} and $S_{\sigma^{-1}(k_\nu)}$ and the transversal $T_{\sigma^{-1}(k_\nu)+1,k_\nu}$. The rest of the $\Sigma_{k_\nu,j_\nu}(\xi_i)$ is divided into triangles. The triangles have 3 E_ℓs as vertices (at least one even and odd) and two transversals and one homoclinic separatrix as edges. There are several ways to do this, but the important thing to demand is that the triangles must be disjoint (except for possibly shared edges) and cover the area. There can be two types of triangles: one type with an edge contained in a clockwise H-chain and one type with an edge contained in a counter-clockwise H-chain (see Figure 14). We number these triangles from left to right as $\Sigma^m_{k_\nu,j_\nu}(\xi_i)$, $m = 1,\ldots,n$. For simplicity of notation, let α_1 be the analytic invariant associated to $Z^{\alpha\omega}_{k_\nu,j_\nu}(\xi_1)$ and α_2 the analytic invariant associated to $Z^{\alpha\omega}_{k_\nu,j_\nu}(\xi_2)$. We define A_0 on $\Sigma^0_{k_\nu,j_\nu}(\xi_1)$ so that

$$\begin{bmatrix} 1 \\ 0 \end{bmatrix} \mapsto \begin{bmatrix} 1 \\ 0 \end{bmatrix} \quad \text{and} \quad \begin{bmatrix} \Re(\alpha_1^-) \\ \Im(\alpha_1^-) \end{bmatrix} \mapsto \begin{bmatrix} \Re(\alpha_2^-) \\ \Im(\alpha_2^-) \end{bmatrix}, \tag{77}$$

and we define A_{n+1} on $\Sigma^{n+1}_{k_\nu,j_\nu}(\xi_1)$ so that

$$\begin{bmatrix} 1 \\ 0 \end{bmatrix} \mapsto \begin{bmatrix} 1 \\ 0 \end{bmatrix} \quad \text{and} \quad \begin{bmatrix} \Re(\alpha_1^+) \\ \Im(\alpha_1^+) \end{bmatrix} \mapsto \begin{bmatrix} \Re(\alpha_2^+) \\ \Im(\alpha_2^+) \end{bmatrix}, \tag{78}$$

so that

$$\underline{A} = \begin{bmatrix} 1 & \frac{\Re(\alpha_2^{\pm}-\alpha_1^{\pm})}{\Im(\alpha_1^{\pm})} \\ 0 & \frac{\Im(\alpha_2^{\pm})}{\Im(\alpha_1^{\pm})} \end{bmatrix} \tag{79}$$

and

$$A_0(x+iy) = x + \frac{\Re(\alpha_2^{-} - \alpha_1^{-})}{\Im(\alpha_1^{-})}y + i\frac{\Im(\alpha_2^{-})}{\Im(\alpha_1^{-})}y \tag{80}$$

$$A_{n+1}(x+iy) = x + \frac{\Re(\alpha_2^{+} - \alpha_1^{+})}{\Im(\alpha_1^{+})}y + i\frac{\Im(\alpha_2^{+})}{\Im(\alpha_1^{+})}y + \mathcal{T}, \tag{81}$$

where $\mathcal{T} = \tau_{\{[\sigma^{-1}(j_\nu)+1]\}}(\xi_2) - \tau_{\{[\sigma^{-1}(j_\nu)+1]\}}(\xi_1)$ is the appropriate positive real constant. Now let

$$v_{\tilde{k}\tilde{j}}(\xi_i) = \alpha_i^{-} + \sum_{j'=\tilde{j}}^{\sigma(j-1)} \tau\left(S_{j',\sigma(j')}(\xi_i)\right) - \sum_{k'=\sigma^{-1}(j)+1}^{\sigma(\tilde{k}-1)} \tau\left(S_{k',\sigma(k')}(\xi_i)\right). \tag{82}$$

Then on each triangle $\Sigma^m_{k_\nu,j_\nu}(\xi_1)$, $m = 1,\dots,n$, with $v_{\tilde{k}\tilde{j}}(\xi_1)$ as the left edge and $S_{\tilde{j}-1,\sigma(\tilde{j}-1)}(\xi_1)$ as the upper (or $S_{\tilde{k},\sigma(\tilde{k})}(\xi_1)$ as the lower) edge, we define A_m by

$$\begin{bmatrix} \tau\left(S_{\ell,\sigma(\ell)}(\xi_1)\right) \\ 0 \end{bmatrix} \mapsto \begin{bmatrix} \tau\left(S_{\ell,\sigma(\ell)}(\xi_2)\right) \\ 0 \end{bmatrix} \quad \text{and} \quad \begin{bmatrix} \Re(v_{\tilde{k}\tilde{j}}(\xi_1)) \\ \Im(v_{\tilde{k}\tilde{j}}(\xi_1)) \end{bmatrix} \mapsto \begin{bmatrix} \Re(v_{\tilde{k}\tilde{j}}(\xi_2)) \\ \Im(v_{\tilde{k}\tilde{j}}(\xi_2)) \end{bmatrix}, \tag{83}$$

$\ell = \tilde{k}, \tilde{j}-1$, so that

$$\underline{A} = \begin{bmatrix} \frac{\tau\left(S_{\ell,\sigma(\ell)}(\xi_2)\right)}{\tau\left(S_{\ell,\sigma(\ell)}(\xi_1)\right)} & \frac{\Re(v_{\tilde{k}\tilde{j}}(\xi_1)-v_{\tilde{k}\tilde{j}}(\xi_1))}{\Im(v_{\tilde{k}\tilde{j}}(\xi_1))} \\ 0 & \frac{\Im(v_{\tilde{k}\tilde{j}}(\xi_2))}{\Im(v_{\tilde{k}\tilde{j}}(\xi_1))} \end{bmatrix} \tag{84}$$

and

$$A_m(x+iy) = x + \frac{\Re(v_{\tilde{k}\tilde{j}}(\xi_2) - v_{\tilde{k}\tilde{j}}(\xi_1))}{\Im(v_{\tilde{k}\tilde{j}}(\xi_1))}y + i\frac{\Im(v_{\tilde{k}\tilde{j}}(\xi_2))}{\Im(v_{\tilde{k}\tilde{j}}(\xi_1))}y + \mathcal{T}_m, \quad m = 1,\dots,n, \tag{85}$$

where $\mathcal{T}_m$ is the proper translation as above.

Every above map is an orientation-preserving linear map and is hence a quasi-conformal homeomorphism. Since each ϕ_1, ϕ_2 is a conformal isomorphism, then the compositions

$$\phi_2^{-1} \circ A \circ \phi_1 \tag{86}$$

are quasi-conformal on the $Z^c \setminus \{\zeta_c\}$, Z^s, and $Z^{\alpha\omega}$. These maps extend continuously to the equilibrium points $\zeta(\xi_i)$. □

Corollary 5.2. *Suppose ξ_1, $\xi_2 \in \Xi_d$ have the same combinatorial and analytic invariants, i.e. $(\sim_1, H_1) = (\sim_2, H_2)$ and $A(\xi_1) = A(\xi_2)$. Then $\xi_1 = \xi_2$ (i.e. $P_1 = P_2$).*

Proof. When the analytic invariants are identical, each $A = \mathrm{id}$ above, and in this case we can conclude that ψ is a holomorphic automorphism of $\mathbb{C}$. The only isomorhpisms ψ that conjugate vector fields in Ξ_d are of the form $z \mapsto \sqrt[d-1]{1}z$. Since both $s_0(\xi_1)$ and $s_0(\xi_2)$ are asymptotic to $\mathbb{R}_+$ at infinity, it follows that ψ is the identity. □

Therefore, the combinatorial and analytic invariants assigned to a vector field determine the vector field uniquely in Ξ_d.

6 The Structure Theorem

We have defined analytic and combinatorial invariants, given a vector field. We now wish to show that given a combinatorial invariant and a set of analytic invariants with the properties described above, there exists a unique polynomial vector field $\xi_P \in \Xi_d$ realizing the given invariants.

Theorem 6.1 (Structure Theorem)**.** *Given a combinatorial data set* $(\sim, H) \in \mathcal{D}_d$ *and an analytic data set* $A \in \mathcal{A}(\sim, H)$*, there exists a unique* $\xi_P \in \Xi_d$ *realizing* $(\sim, H)$ *and* A*, i.e.* $(\sim_P, H_P) = (\sim, H)$ *and* $A(\xi_P) = A$*.*

The proof is constructed as follows:

1. Construct the *rectified surface* $\mathcal{M}$ with vector field $\xi_{\mathcal{M}}$ from the data $(\sim, H)$ and A.
2. Define an atlas on $\mathcal{M}$ to show it is a Riemann surface
3. Show that $\mathcal{M}$ is isomorphic to $\hat{\mathbb{C}}$.
4. Show existence of the unique isomorphism $\Phi : \mathcal{M} \to \hat{\mathbb{C}}$ that induces $\Phi_*(\xi_{\mathcal{M}}) = \xi_P \in \Xi_d$ having the given invariants.

7 Definition of and Atlas for $\mathcal{M}$

Let $(\sim, H)$ (a combinatorial data set) and $\mathcal{A}(\sim, H)$ (a corresponding total analytic invariant) be given. Out of these data, we will construct a Riemann surface $\mathcal{M}$ with a vector field $\xi_{\mathcal{M}}$.

7.1 Construction of the Rectified Space

We first construct the rectified zones: vertical half-strips, half-planes, and strips as follows.

For every counter-clockwise (respectively clockwise) closed H-chain $H_{\{[k_{i_1}]\}}$ (resp. $H_{\{[j_{i_1}]\}}$), we construct an upper (lower) vertical half-strip

$$C_{\{[k_{i_1}]\}} = \Big\{ z \in \mathbb{H} \mid 0 < \Re(z) < \tau_{\{[k_{i_1}]\}} \Big\}$$

$$\Big(\text{resp. } C_{\{[j_{i_1}]\}} = \Big\{ z \in -\mathbb{H} \mid 0 < \Re(z) < \tau_{\{[j_{i_1}]\}} \Big\}\Big)$$

Its lower (resp. upper) boundary is $]0, \tau_{\{[k_{i_1}]\}}[\subset \mathbb{R}$ (resp. $]0, \tau_{\{[j_{i_1}]\}}[\subset \mathbb{R}$), labeled according to the corresponding H-chain as in Definition 3.8. That is, $]0, \tau(S_{k_{i_1},\sigma(k_{i_1})})[$ (resp. $]0, \tau(S_{j_{i_n},\sigma(j_{i_n})})[$) is labeled by $S_{k_{i_1},\sigma(k_{i_1})}$ (resp. $S_{j_{i_n},\sigma(j_{i_n})}$), and

$$]\tau(S_{k_{i_1},\sigma(k_{i_1})}), \tau(S_{k_{i_1},\sigma(k_{i_1})}) + \tau(S_{k_{i_2},\sigma(k_{i_2})})[$$

$$\Big(\text{resp. }]\tau(S_{j_{i_n},\sigma(j_{i_n})}), \tau(S_{j_{i_n},\sigma(j_{i_n})}) + \tau(S_{j_{i_{n-1}},\sigma(j_{i_{n-1}})})[\Big)$$

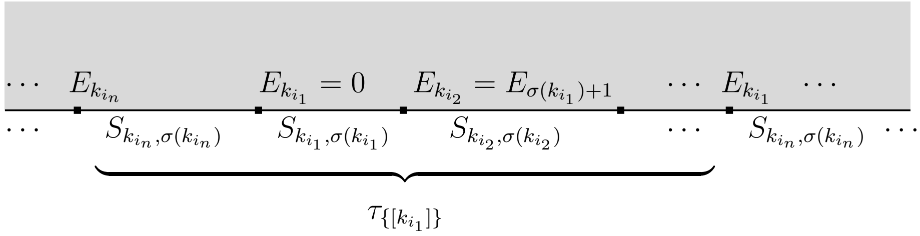

$\cdots$ $E_{k_{i_n}}$ $E_{k_{i_1}} = 0$ $E_{k_{i_2}} = E_{\sigma(k_{i_1})+1}$ $\cdots$ $E_{k_{i_1}}$ $\cdots$
$\cdots$ $S_{k_{i_n},\sigma(k_{i_n})}$ $S_{k_{i_1},\sigma(k_{i_1})}$ $S_{k_{i_2},\sigma(k_{i_2})}$ $\cdots$ $S_{k_{i_n},\sigma(k_{i_n})}$ $\cdots$
$\tau_{\{[k_{i_1}]\}}$

Figure 15: Depiction of how to build an upper vertical half-strip from a counter-clockwise closed H-chain.

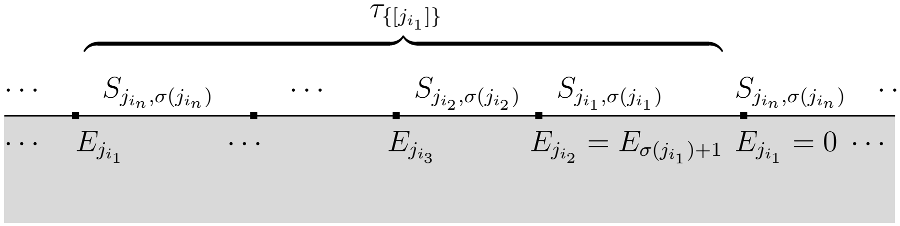

$\tau_{\{[j_{i_1}]\}}$
$\cdots$ $S_{j_{i_n},\sigma(j_{i_n})}$ $\cdots$ $S_{j_{i_2},\sigma(j_{i_2})}$ $S_{j_{i_1},\sigma(j_{i_1})}$ $S_{j_{i_n},\sigma(j_{i_n})}$ $\cdots$
$\cdots$ $E_{j_{i_1}}$ $\cdots$ $E_{j_{i_3}}$ $E_{j_{i_2}} = E_{\sigma(j_{i_1})+1}$ $E_{j_{i_1}} = 0$ $\cdots$

Figure 16: Depiction of how to build a lower vertical half-strip from a clockwise closed H-chain.

is labeled as in Definition 3.9 by $S_{k_{i_2},\sigma(k_{i_2})}$ (resp. $S_{j_{i_{n-1}},\sigma(j_{i_{n-1}})}$), etc. (see Figure 15 resp. Figure 16). Each homoclinic separatrix $S_{k,j}$ in the H-chain connects the marked points E_k and E_{j+1} (resp. E_{k-1} and E_j) in $\mathbb{R}$.

For every counter-clockwise (resp. clockwise) open H-chain $H_{\{[k_{i_1}]\}}$ (resp. $H_{\{[j_{i_1}]\}}$) of length $n \geq 0$, the odd separatrix S_k, $k = \sigma(k_{i_n})+1$ (resp. $k = j_{i_n}-1$), and the even separatrix S_j, $j = k_{i_1}-1$ (resp. $j = \sigma(j_{i_1})+1$), are attached to the H-chain by the ends E_k and E_{j+1} (resp. E_{k+1} and E_j) respectively. If $k = \sigma(j)$ (resp. $j = \sigma(k)$), then there are two possibilities: either the H-chain together with S_k, S_j, and all the ends they connect make up the lower (resp. upper) boundary of an upper (resp. lower) half-plane $\mathbb{H}_k$ (resp. $-\mathbb{H}_j$), or they are on the lower (resp. upper) boundary of the strip $\Sigma_{k,\sigma(j)}$ (resp. $\Sigma_{\sigma(k),j}$), where $S_{\sigma(j)}$ and $S_{\sigma^{-1}(k)}$ (resp. $S_{\sigma^{-1}(j)}$ and $S_{\sigma(k)}$) are attached to the same open H-chain, and these together with the ends they connect make up the upper (resp. lower) boundary of the strip.

In the case of a strip $\Sigma_{k,j}$, we label $\mathbb{R}_-$ by $S_{\sigma^{-1}(j)}$, and we label $\mathbb{R}_- + \alpha_i^-(\sim, H)$ by S_j ($\tau := 0$ when the H-chain has length 0). Now S_j and $S_{\sigma^{-1}(j)}$ are attached to the clockwise, respectively counter-clockwise, open H-chains $H_{\{[\sigma(j-1)]\}}$ and $H_{\{[\sigma^{-1}(j)+1]\}}$. The interval $[0, \tau_{\{[\sigma^{-1}(j)+1]\}}]$ is labelled by the homoclinic separatrices in $H_{\{[\sigma^{-1}(j)+1]\}}$ and the ends they connect, and $[0, \tau_{\{[\sigma(j-1)]\}}] + \alpha_i^-(\sim, H)$ is labelled by the homoclinic separatrices in $H_{\{[\sigma(j-1)]\}}$ and the ends they connect. Finally, $]\tau_{\{[\sigma^{-1}(j)+1]\}}, \infty[$ is labelled by S_k, and $]\tau_{\{[\sigma(j-1)]\}}, \infty[+ \alpha_i^-(\sim, H)$ is labelled by $S_{\sigma^{-1}(k)}$ (see Figure 17).

Every separatrix is on the upper boundary of exactly one rectified zone and on the lower boundary of exactly one rectified zone. In the non-homoclinic case, it is on the boundary of:

- two strips,

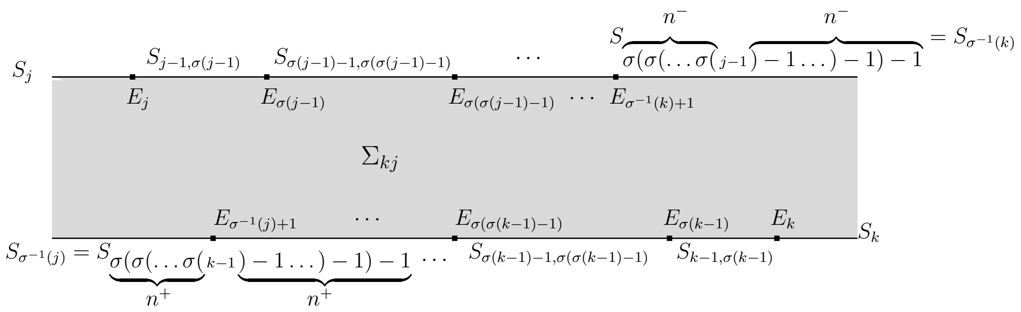
n^-
n^-
$S_{\sigma(\sigma(\dots\sigma(j-1)-1\dots)-1)-1} = S_{\sigma^{-1}(k)}$
S_j
$S_{j-1,\sigma(j-1)}$
$S_{\sigma(j-1)-1,\sigma(\sigma(j-1)-1)}$
$\cdots$
E_j
$E_{\sigma(j-1)}$
$E_{\sigma(\sigma(j-1)-1)}$
$\cdots$
$E_{\sigma^{-1}(k)+1}$
Σ_{kj}
$E_{\sigma^{-1}(j)+1}$
$\cdots$
$E_{\sigma(\sigma(k-1)-1)}$
$E_{\sigma(k-1)}$
E_k
S_k
$S_{\sigma^{-1}(j)} = S_{\sigma(\sigma(\dots\sigma(k-1)-1\dots)-1)-1}$
$\cdots$
$S_{\sigma(k-1)-1,\sigma(\sigma(k-1)-1)}$
$S_{k-1,\sigma(k-1)}$
n^+
n^+

Figure 17: Depiction of how to build a strip with one clockwise and one counterclockwise H-chain on the boundary. The construction is the same for open H-chains on the boundaries of half-planes.

- one strip and one half-plane, or
- two half-planes (see Figure 28).

In the homoclinic separatrix case, the separatrix is on the boundary of:

- two strips,
- one strip and one half-plane (see Figure 25),
- one strip and one vertical half-strip (see Figure 26),
- two half-planes (see Figure 24),
- one half-plane and one vertical half-strip, or
- two vertical half-strips (see Figure 27).

Every separatrix admits a unit-speed parameterization, one starting from the marked point labeled by E_ℓ and the other from $E_{\ell+1}$ always such that if E_j is seen from below, then E_{j+1} is seen from above corresponding to the ends on either side of S_j, and if E_{k+1} is seen from below, then E_k is seen from above corresponding to the ends on either side of S_k (compare Figures 15 and 16).

Now that we have constructed the vertical half strips $C_{\{[\ell]\}}$, half-planes $\pm\mathbb{H}_\ell$, and strips $\Sigma_{k,j}$ with proper labeling,

$$\mathcal{M}^* = \left(\coprod \overline{C}_{\{[\ell]\}} \coprod \pm\overline{\mathbb{H}}_\ell \coprod \overline{\Sigma}_{k,j}\right) / \sim, \tag{87}$$

where $\sim$ is the equivalence relation such that all ends are identified, $E = \{E_\ell\}/\sim$, each pair of points $z \in S_\ell$ or $z \in S_{k,j}$ on the two occurences of any separatrix respecting the unit-speed parameterization are identified, and $z \sim z + \tau_{\{[\ell]\}}$ for $z \in i\mathbb{R}_{\geq 0} \subset \partial C_{\{[\ell]\}}$.

Proposition 7.1. *The set $\mathcal{M}^*$ is a Hausdorff topological space.*

Proof. Each $\overline{C}_{\{[\ell]\}}$, $\pm\overline{\mathbb{H}}_\ell$, and $\overline{\Sigma}_{k,j}$ is a Hausdorff topological space with subspace topology from $\mathbb{C}$. Every disjoint union of Hausdorff spaces is again Hausdorff, so the disjoint union $\coprod \overline{C}_{\{[\ell]\}} \coprod \pm\overline{\mathbb{H}}_\ell \coprod \overline{\Sigma}_{k,j}$ is a Hausdorff topological space. Now $\mathcal{M}^*$ is a topological space with the quotient topology, and one can convince oneself that the identified points under $\sim$ do not cause any separability problems. $\square$

As a topological space, $\mathcal{M}^*$ has q ends we call $\infty_{[\ell]}$ corresponding to the equivalence classes $[\ell] \in L$ and $c = c(\sim, H)$ ends $\infty_{\{[\ell]\}}$ corresponding to the closed H-chains $H_{\{[\ell]\}}$. We will make charts of the neighborhoods of the ends to show that each end corresponds to one point. The natural $(q+c)$-point closure of $\mathcal{M}^*$ is denoted $\mathcal{M}$ and is called the *rectified surface*. The construction of the Riemann surface structure on $\mathcal{M}$ is contained in the construction of the atlas that follows.

7.2 An atlas for $\mathcal{M}$

We show that $\mathcal{M}$ is a Riemann surface by constructing an atlas for $\mathcal{M}$. We construct overlapping open sets $U \subset \mathcal{M}$ covering $\mathcal{M}$, and define charts $\eta_U : U \to \mathbb{C}$. There are four types of points on $\mathcal{M}$ we need to consider:

- points in rectified zones,
- points on separatrices,
- the point E, and
- the ends of $\mathcal{M}^*$.

For the first type of point, we only need to note that each $C_{\{[\ell]\}}$, $\pm\mathbb{H}_\ell$, and $\Sigma_{k,j}$ has as a natural chart in $\mathbb{C}$ by projection.

For points on separatrices, we note the following. Since each separatrix is on the upper boundary of exactly one rectified zone and on the lower boundary of exactly one rectified zone, we let U in the non-homoclinic case be the open set in $\mathcal{M}^*$ which corresponds to the two rectified zones in $\mathbb{C}$ identified along S_ℓ and let $\eta_U : U \to \mathbb{C}$ be the chart for which $\eta_U(S_\ell) = \mathbb{R}_+$ (resp. $\mathbb{R}_-$) for ℓ odd (resp. even). In the homoclinic case, we let U be the open set in $\mathcal{M}^*$ which corresponds to the two rectified zones in $\mathbb{C}$ identified along $S_{k,j} \subseteq]0, \tau[$, where τ is the length of $S_{k,j}$.

We define a chart $\eta_E : U_E \to \mathbb{D}_{\frac{\sqrt[d-1]{r}}{d-1}}$ around E as follows.

For each ℓ, let D_ℓ be the semi-disk in either a strip, half-plane, or vertical half-strip with center E_ℓ, "positive" (see Figure 18) if ℓ is odd, "negative" if ℓ is even, and with radius r sufficiently small, i.e.

$$r < \frac{1}{2}\left(\min_i\{\Im(\alpha_i(\sim, H))\}, \{\tau_i(\sim, H)\}\right) \tag{88}$$

for $i = 1, \ldots, s$, and $i = 1, \ldots, h$, respectively (see Figures 18 and 20). The neighborhood $U_E \subset \mathcal{M}$ of E is then the half-disks taken with proper identification, $\{D_\ell\}/\sim$.

First consider the map $E \mapsto 0$, giving a $d-1$ covering of $\mathbb{D}_r$ corresponding to $\arg(Z - E_\ell) \in [-(\ell-1)\pi, -(\ell-2)\pi]$ in each D_ℓ. To get a univalent covering, we apply the appropriate $(d-1)^{st}$ root by setting $\phi_E : \mathbb{D}_r \to \mathbb{D}_{\frac{\sqrt[d-1]{r}}{d-1}}$, where

$$\phi_E(z) = \exp\left(\frac{1}{d-1}\mathcal{L}_{(-\ell+\frac{1}{2})\pi}\right) \tag{89}$$

and $\mathcal{L}_{(-\ell+\frac{1}{2})\pi}$ is an appropriate branch of the logarithm. This takes our $d-1$ covering about 0 to a univalent covering of $\mathbb{D}_{\frac{\sqrt[d-1]{r}}{d-1}}$ where S_0 is asypmtotic to $\mathbb{R}_+$ at infinity (see Figure 19).

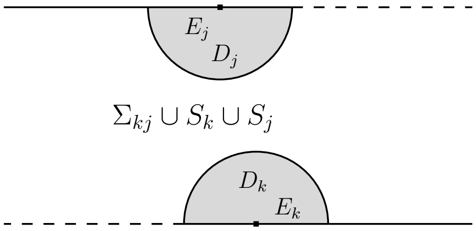

Figure 18: Half disks D_k^+ and D_j^-.

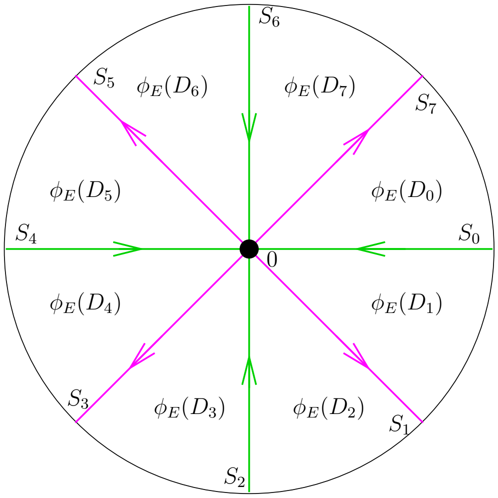

Figure 19: A neighborhood of $\eta_E(E) = 0$ in the chart η_E exemplified for $d = 5$.

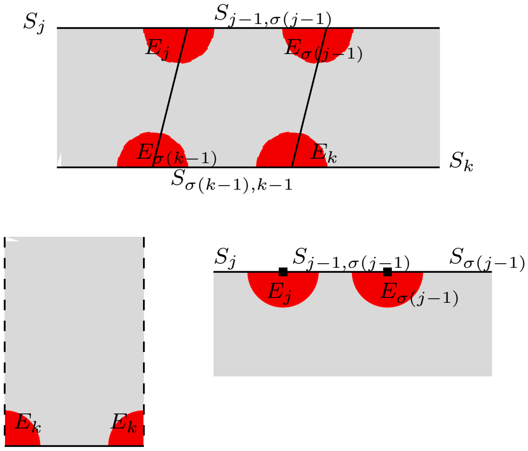

Figure 20: Examples of how one can construct half-disks for the ends in each rectified zone.

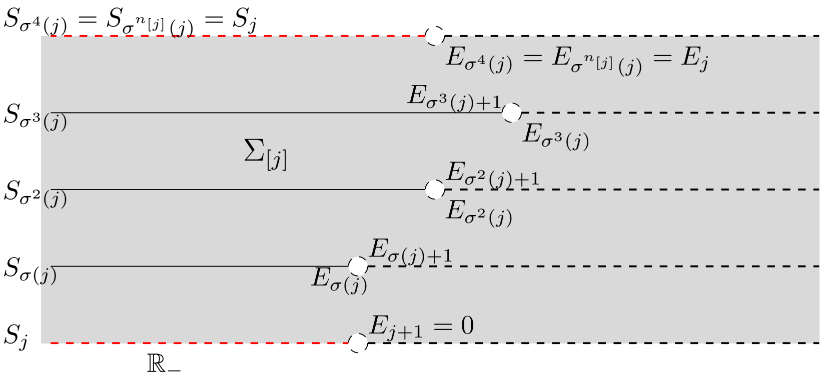

Figure 21: Example of the set $\Sigma_{[j]}$ for an even equivalence class with four elements.

We now construct overlapping open sets $U \subset \mathcal{M}$ covering the ends of $\mathcal{M}^*$, and define charts $\eta_U : U \to \mathbb{C}$ determined by $\rho_{[\ell]}$ for each odd or even equivalence class and closed H-chain. The chart about mixed equivalence classes is constructed via Fatou coordinates.

7.3 Neighborhoods of odd or even equivalence classes and closed H-chains

Let $\Sigma_{[\ell]}$ be the open set in $\mathbb{C}$ corresponding to an odd or even equivalence class $[\ell]$ constructed in the following manner.

Let $I_{[\ell]} = \{i \in 1, \dots, s(\sim, H) \mid j_i \in [\ell]\}$.

For an even equivalence class $[j]$ (see Figure 21), we make an open strip in the plane $\{z \in \mathbb{C} \mid 0 < \Im(z) < \Im(\rho_{[j]})\}$. We take away the half line $\{z \in \mathbb{C} \mid z = \alpha_i^-(\sim, H) + t, \quad t \in \mathbb{R}_+\}$ such that $i \in I_{[j]}$. We continue this process for the remainder of $j \in [j]$.

For an odd equivalence class $[k]$ (see Figure 22), we make an open strip in the plane $\{z \in \mathbb{C} \mid 0 < \Im(z) < \Im(\rho_{[k]})\}$. We take away the half line $\{z \in \mathbb{C} \mid z = \alpha_i^+(\sim, H) + t, \quad t \in \mathbb{R}_-\}$. We continue this process for the remainder of $k \in [k]$ (see Figure 22).

We first define $U^*_{[\ell]} = (\Sigma_{[\ell]}/\sim)$, where $\sim$ means identifying the appropriate points of S_ℓ. We define for $[\ell]$ odd (respectively, $[\ell]$ even) $\tilde{U}_{[\ell]} = U^*_{[\ell]} \setminus S_\ell$. Now $\tilde{U}_{[\ell]}$ is an open subset in $\mathcal{M}^*$, which is identified by $q_{[\ell]} : \tilde{U}_{[\ell]} \to \Sigma_{[\ell]}$ with the open set $\Sigma_{[\ell]} \subset \mathbb{C}$. This domain in $\mathbb{C}$ is then mapped by $\phi_{[\ell]} : \Sigma_{[\ell]} \to \mathbb{C}$ defined by $\phi_{[\ell]}(Z) = \exp\left(\frac{\mp 2\pi i}{\rho_{[\ell]}} Z\right)$. The image $\phi_{[\ell]}(\Sigma_{[\ell]})$ is $\mathbb{C}$ except for one complete logarithmic spiral going through the point $z = 0$, the origin, and tails of logarithmic spirals corresponding to $\phi_{[\ell]}(\partial\Sigma_{[\ell]})$. Note that $\partial\Sigma_{[\ell]}$ consists of all the dotted lines in Figures 21 and 22 along with the E_{ℓ_i} and E_{ℓ_i+1} where $\ell_i \in [\ell]$. The map $\phi_{[\ell]}$ extends continuously to $\varphi_{[\ell]} : \Sigma_{[\ell]} \cup \mathbb{R}_\pm \to V^*_{[\ell]}$ where $V^*_{[\ell]}$ is $\mathbb{C}$ minus the origin and tails of logarithmic spirals corresponding to $\partial\Sigma_{[\ell]} \setminus \{\mathbb{R}_\pm \cup (\rho_{[\ell]} + \mathbb{R}_\pm)\}$ (see Figure 23). It is defined as follows:

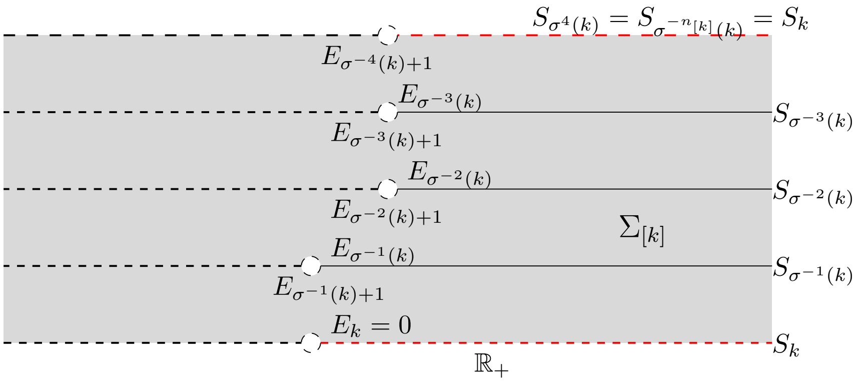

Figure 22: Example of the set $\Sigma_{[k]}$ for an odd equivalence class with four elements.

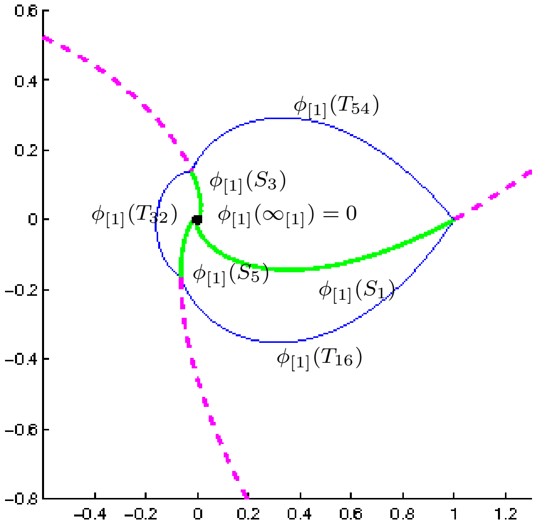

Figure 23: $V_{[k]}$ for an odd equivalence class $[k]$. Specifically, $[1] = \{1, 3, 5\}$. The thin dark curves are the images of the rectified transversals T_{16}, T_{32}, and T_{54} under $\phi_{[1]}$. The solid light curves are the images of the rectified separatrices S_1, S_3, and S_5. The dashed curves are tails of logarithmic spirals which are the images of $\mathbb{R}_-$, $\mathbb{R}_- + \alpha^+_{i_3}$, $\mathbb{R}_- + \alpha^+_{i_3} + \alpha^+_{i_2}$, and $\mathbb{R}_- + \alpha^+_{i_3} + \alpha^+_{i_2} + \alpha^+_{i_1}$, where $i_2 = i_1 + 1$ and $i_3 = i_2 + 1$.

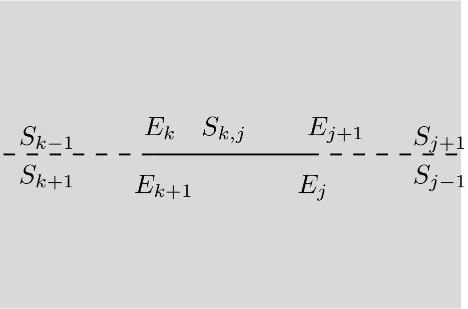

Figure 24: The neighborhood of an equivalence class in H on the rectified surface $\mathcal{M}$ in the case where the neighborhood consists of two half-planes, along with the line segment corresponding to the equivalence class.

$$\varphi_{[\ell]}(Z) = \begin{cases} \phi_{[\ell]} & \text{for } Z \in \Sigma_{[\ell]} \\ \exp\left(\frac{\mp 2\pi i}{\rho_{[\ell]}} Z\right) & \text{for } Z \in \mathbb{R}_{\pm} \end{cases}. \tag{90}$$

For an even or odd equivalence class $[\ell]$, we define $\eta_{[\ell]} : U^*_{[\ell]} \to V^*_{[\ell]}$ by $\eta_{[\ell]} = \varphi_{[\ell]} \circ q_{[\ell]}$ $(Z \neq 0)$. This is a chart on $U^*_{[\ell]}$ which can be extended to a chart $\eta_{[\ell]} : U_{[\ell]} \to V_{[\ell]}$ on $U_{[\ell]}$ by mapping the puncture $\infty_{[\ell]} \mapsto 0$.

The next case corresponds to a closed H-chain $H_{\{[\ell]\}}$, where we remind that clockwise or counter-clockwise orientation are represented by ℓ even or odd respectively. We define $U^*_{\{[\ell]\}}$ to be the open set on $\mathcal{M}$, constructed by $C_{\{[\ell]\}}/\sim$. We define for $[\ell]$ odd (respectively, $[\ell]$ even) $\tilde{U}_{\{[\ell]\}} = U^*_{\{[\ell]\}} \backslash S$ where S is the curve on $\mathcal{M}$ defined by the equivalence relation $z \sim z + \tau_{\{[\ell]\}}$, $z \in i\mathbb{R}_{\pm} \subset \partial C_{\{[\ell]\}}$. Now $\tilde{U}_{\{[\ell]\}}$ is an open subset in $\mathcal{M}$, which is identified by $q_{\{[\ell]\}} : \tilde{U}_{\{[\ell]\}} \to C_{\{[\ell]\}}$ with the open set $C_{\{[\ell]\}} = \{z \in \pm\mathbb{H} \mid 0 < \Re(z) < \tau_{\{[\ell]\}}\}$. This domain $C_{\{[\ell]\}} \subset \mathbb{C}$ is then mapped by $\phi_{\{[\ell]\}} : C_{\{[\ell]\}} \to \mathbb{D}$ defined by $\phi_{\{[\ell]\}}(Z) = \exp\left(\frac{\mp 2\pi i}{\tau_{\{[\ell]\}}} Z\right)$. The image is $\phi_{\{[\ell]\}}\left(C_{\{[\ell]\}}\right) = \mathbb{D} \setminus [0, 1[$. The map $\phi_{\{[\ell]\}}$ extends continuously to $\phi_{\{[\ell]\}} : C_{\{[\ell]\}} \cup i\mathbb{R}_{\pm} \to \mathbb{D}^*$. It is defined as follows:

$$\varphi_{\{[\ell]\}}(Z) = \begin{cases} \phi_{\{[\ell]\}} & \text{for } Z \in C_{\{[\ell]\}} \\ \exp\left(\frac{\mp 2\pi i}{\tau_{\{[\ell]\}}} Z\right) & \text{for } Z \in i\mathbb{R}_{\pm} \end{cases}. \tag{91}$$

For $[\ell]$ odd (resp. even), we define $\eta_{\{[\ell]\}} : U^*_{\{[\ell]\}} \to \mathbb{D}^*$ by $\eta_{\{[\ell]\}} = \varphi_{\{[\ell]\}} \circ q_{\{[\ell]\}}$ $(Z \neq 0)$. This is a chart which extends to $\eta_{\{[\ell]\}} : U_{\{[\ell]\}} \to \mathbb{D}$ by $\infty_{\{[\ell]\}} \mapsto 0$.

7.4 Neighborhoods around Mixed Equivalence Classes $[m]$

For a mixed equivalence class $[m]$ with $p_{[m]}$ parity changes, we define $U^*_{[m]}$ to be a suitably restricted domain on $\mathcal{M}^*$, identified with appropriate restrictions (to be determined below) of upper and lower half-planes $\mathbb{H}_k$ and $-\mathbb{H}_j$ with $k \sim j \in [m]$ and half-strips of the $\Sigma_{k,j}$ such that either $j \sim \sigma^{-1}(j) \in [m]$ or $k \sim \sigma^{-1}(k) \in [m]$, with proper identification along the separatrices. The goal is to show the existence of a chart $\eta_{[m]} : U^*_{[m]} \to V^*_{[m]}$, where $V_{[m]}$ is some neighborhood of 0, and the puncture $\infty_{[m]}$ in $U^*_{[m]}$ corresponds to 0.

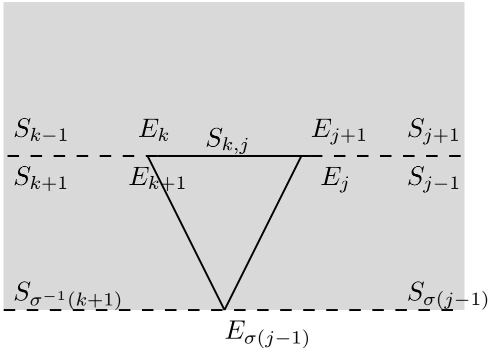

Figure 25: The neighborhood of an equivalence class in H on the rectified surface $\mathcal{M}$ in the case where the neighborhood of the equivalence class consists of one half-plane, a strip, and the line segment corresponding to the equivalence class.

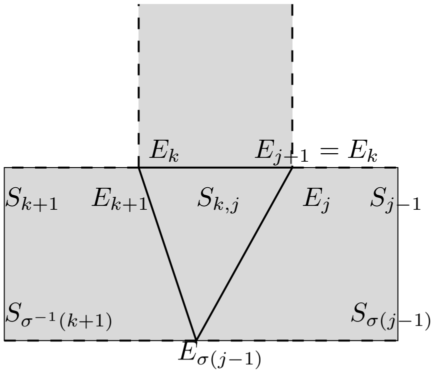

Figure 26: The neighborhood of an equivalence class in H on the rectified surface $\mathcal{M}$ in the case where the neighborhood of the equivalence class consists of one vertical half-strip sewn to the strip along the line segment corresponding to the equivalence class.

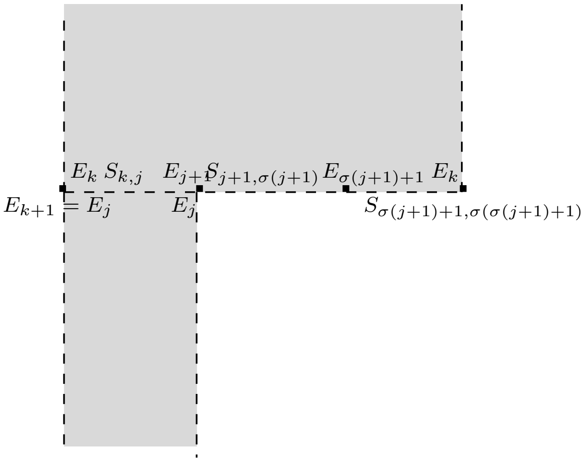

Figure 27: The neighborhood of an equivalence class in H on the rectified surface $\mathcal{M}$ in the case where the equivalence class belongs to two different closed H-chains. The neighborhood of the equivalence class consists of an upper and lower vertical half-strip, possibly having different widths, along with the line segment corresponding to the equivalence class.

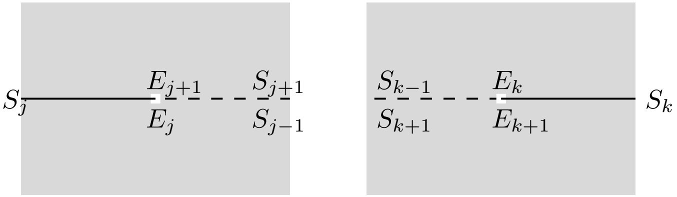

Figure 28: The figure on the left is a neighborhood of a separatrix S_j, $j \in [m]$. It consists of an upper and lower half-plane sewn along the separatrix S_j, so it can be represented by $\mathbb{C} \setminus (\mathbb{R}_+ \cup \{0\})$. The figure on the right is a neighborhood of a separatrix S_k, $k \in [m]$. It consists of an upper and lower half-plane sewn along the separatrix S_k, so it can be represented by $\mathbb{C} \setminus (\mathbb{R}_- \cup \{0\})$.

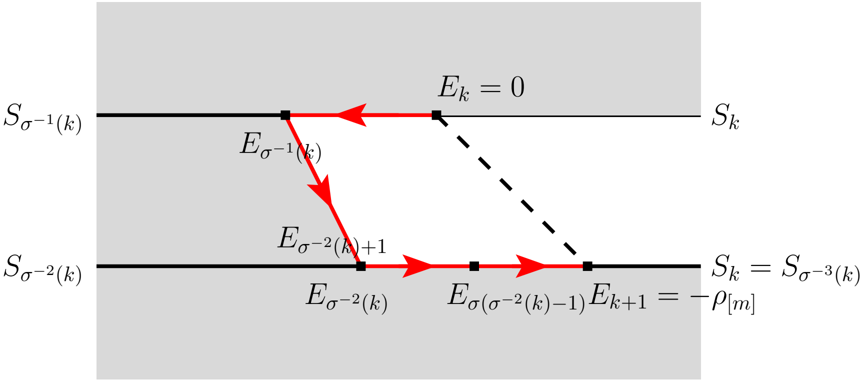

Figure 29: Possible depiction of an almost $p_{[m]}/2$ times "covering" of ∞ in rectifying coordinates with $\Im\left(\rho_{[m]}\right) > 0$ and $p_{[m]} = 2$.

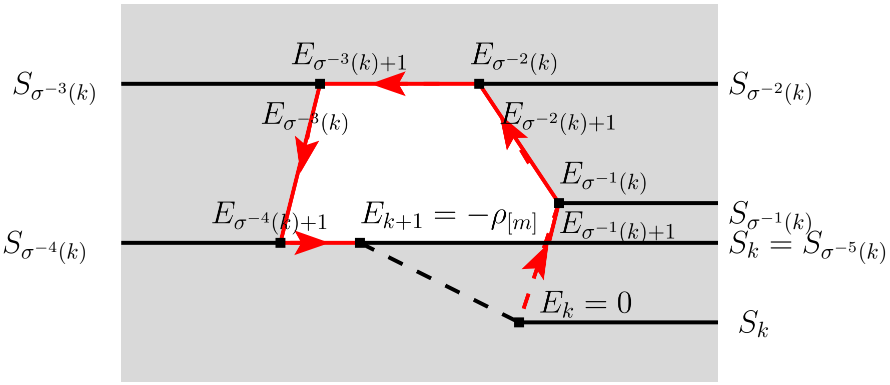

Figure 30: Possible depiction of a more than $p_{[m]}/2$ times "covering" of ∞ in rectifying coordinates with $\Im\left(\rho_{[m]}\right) < 0$ and $p_{[m]} = 2$.

Pick some $k \in [m]$ and fix in $\mathbb{C}$ the half-plane or half-strip having S_k on its lower boundary such that S_k is equal to $\mathbb{R}_+$. Continue building counterclockwise in this way with identification corresponding to $[m]$ until one comes back to the other represenation of the separatrix S_k on the upper boundary of some half-plane or half-strip, which will be identified with the half-line $\mathbb{R}_+ - \rho_{[m]}$.The half-planes and half-strips will wind around approximately $p_{[m]}/2$ times in the following sense: a neighborhood of ∞ is "covered" $p_{[m]}/2$ times if $\Im\left(\rho_{[m]}\right) = 0$, almost $p_{[m]}/2$ times if $\Im\left(\rho_{[m]}\right) > 0$ (see Figure 29), and a bit more than $p_{[m]}/2$ times if $\Im\left(\rho_{[m]}\right) < 0$ (see Figure 30). Let $\mathbb{D}_R$ be the disk with radius

$$R = \sum_{i=1}^{s} |\alpha_i| + \sum_{i=1}^{h} |\tau_i| \,. \tag{92}$$

Then through several steps we can construct a chart $\eta_{[m]} : U^*_{[m]} \to V^*_{[m]}$. The following steps in the construction of the chart $\eta_{[m]}$ are inspired by Shishikura's treatment of Fatou coordinates in [Shi00].

Consider the map $\pi : \mathbb{C} \to \mathbb{C}$ defined by

$$\pi(z) = \exp\left(\pi i p_{[m]} z\right). \tag{93}$$

Note that $\pi\left(z + \frac{n}{p_{[m]}/2}\right) = \pi(z)$ for all $n \in \mathbb{Z}$.

Set $\gamma' = i\mathbb{R}$, i.e. the unique preimage of $\mathbb{R}_+$ under π such that $\Re(z) = 0$ for $z \in \gamma'$, and let $\tilde{\gamma}'$ be the unique preimage of the half-line $\mathbb{R}_+ - \rho_{[m]}$ under π contained in the strip $\frac{p_{[m]}/2-1}{p_{[m]}/2} < \Re(z) < 1$ when $\Im\left(\rho_{[m]}\right) > 0$ ($1 < \Re(z) < \frac{p_{[m]}/2+1}{p_{[m]}/2}$ when $\Im\left(\rho_{[m]}\right) < 0$, and $\Re(z) = 1$ when $\Im\left(\rho_{[m]}\right) = 0$). Note that in each case $\Re(z) \to 1$ for $\Im(z) \to -\infty$ on $\tilde{\gamma}'$ (see Figure 31).

We define the map $\tilde{f} : \gamma' \to \tilde{\gamma}'$ such that it satisfies

$$\left(\pi \circ \tilde{f}\right)(z) = \pi(z) + \tau, \quad z \in \gamma' \tag{94}$$

with $\tau = -\rho_{[m]}$, i.e. so that the proper identification is preserved. From this

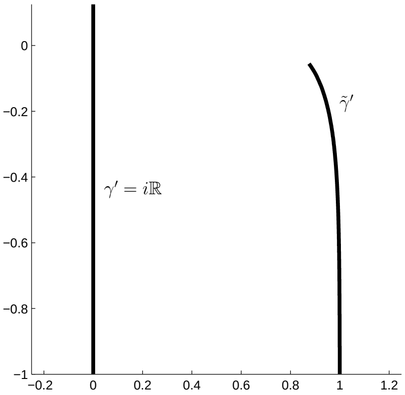

Figure 31: Graph of γ', the unique preimage of $\mathbb{R}_+$ under π such that $\Re(z) = 0$, and $\tilde{\gamma}'$, the unique preimage of the half-line $\mathbb{R}_+ - \rho_{[m]}$ under π for which $\Re(z) \to 1$ for $\Im(z) \to -\infty$ on $\tilde{\gamma}'$. In this example, $\rho_{[m]} = -1 + 2i$ and $p_{[m]} = 2$ (compare with Figure 29), so the preimage contained in the strip $0 < \Re(z) < 1$.

relation, one can deduce the expression

$$\tilde{f}(z) = z + 1 + \frac{\operatorname{Log}\left(1 + \tau \exp\left(-\pi i p_{[m]} z\right)\right)}{\pi i p_{[m]}}, \quad z \in \gamma'. \tag{95}$$

The function $\tilde{f}$ can be extended holomorphically in some lower half plane $H_1 = \{z \in \mathbb{C} \mid \Im(z) < c_1 < 0\}$. The constant c_1 can be determined by forcing the condition $|\tau \exp\left(-\pi i p_{[m]} z\right)| < 1$ so that Log is analytic in H_1. Then c_1 becomes

$$c_1 = \frac{-\ln|\tau|}{\pi p_{[m]}}. \tag{96}$$

Proposition 7.2. *There exists a half-plane $H_2 \subset H_1$ such that $\tilde{f}$ satisfies the properties*

$$|\tilde{f}(z) - (z+1)| < 1/4 \tag{97}$$

$$|\tilde{f}'(z) - 1| < 1/4. \tag{98}$$

Proof. Suppose $|\tau| \exp\left(\pi p_{[m]} \Im(z)\right) < R < 1$ for some R. This can be rewritten as

$$\Im(z) < c_1 + \frac{\ln(R)}{\pi p_{[m]}}, \tag{99}$$

for which we have

$$|\tilde{f}'(z) - 1| = \frac{|-\tau \exp\left(-\pi i p_{[m]} z\right)|}{|1 + \tau \exp\left(-\pi i p_{[m]} z\right)|} \leq \frac{R}{1-R}. \tag{100}$$

For the other condition, we can calculate

$$|\tilde{f}(z) - (z+1)| = \frac{|\operatorname{Log}\left(1 + \tau \exp\left(-\pi i p_{[m]} z\right)\right)|}{|\pi i p_{[m]}|} \tag{101}$$

and $|\mathrm{Arg}\left(1+\tau\exp\left(-\pi i p_{[m]}z\right)\right)| < \mathrm{Arcsin}\left(R\right)$, giving

$$|\tilde{f}\left(z\right)-\left(z+1\right)|^2 < \frac{1}{\left(\pi p_{[m]}\right)^2}\left[\ln^2\left(1+R\right)+\mathrm{Arcsin}^2\left(R\right)\right]. \tag{102}$$

Since $\frac{R}{1-R}$, $\ln\left(1+R\right)$, and $\mathrm{Arcsin}\left(R\right)$ tends to 0 as $R\to 0$, we can conclude that there exists $R<1$ such that $|\tilde{f}\left(z\right)-\left(z+1\right)| < \frac{1}{4}$ and $|\tilde{f}'\left(z\right)-1| < 1/4$. Choose c_2 such that the above conditions are satisfied in the half-plane $H_2 = \{z \mid \Im\left(z\right) < c_2\}$. ☐

Lemma 7.3. *$\tilde{f}$ is univalent in H_2.*

Proof. Take two points $z_1 \neq z_2$ in H_2. We show that $\tilde{f}\left(z_1\right)\neq\tilde{f}\left(z_2\right)$. One can always connect two points in the half-plane H_2 with a straight line segment. We parameterize this line segment by

$$l\left(t\right) = \left(1-t\right)z_1 + tz_2, \quad t\in[0,1]. \tag{103}$$

Let $L\left(t\right)=\tilde{f}\left(l\left(t\right)\right)$. Then

$$\tilde{f}\left(z_2\right)-\tilde{f}\left(z_1\right) = \int_0^1 L'\left(t\right)dt, \tag{104}$$

and since $l'\left(t\right) = z_2 - z_1 \neq 0$ is a constant,

$$\tilde{f}\left(z_2\right)-\tilde{f}\left(z_1\right) = 0 \Leftrightarrow \int_0^1 \tilde{f}'\left(l\left(t\right)\right)dt = 0. \tag{105}$$

But

$$\int_0^1 \Re\left(\tilde{f}'\left(l\left(t\right)\right)\right)dt > 0 \tag{106}$$

by Equation (98), so $\tilde{f}\left(z_2\right)\neq\tilde{f}\left(z_1\right)$. ☐

We now construct a univalent function Φ in a closed region Ω (defined below) satisfying $\Phi\left(\tilde{f}\left(z\right)\right) = \Phi\left(z\right)+1$ on $\gamma = \Omega\cap\gamma'$. Using the same method as in [Shi00], let $\Sigma = \{z \mid 0\leq\Re\left(z\right)\leq 1, \Im\left(z\right)\leq c_3 < c_2\}$ and $\Omega = h_1\left(\Sigma\right)$ where $h_1 : \Sigma\to\Omega$ is defined by

$$h_1\left(x,y\right) = \left(1-x\right)\left(iy\right) + x\tilde{f}\left(iy\right), \quad 0\leq x\leq 1, y\leq c_3. \tag{107}$$

We restrict to $y\leq c_3 < c_2$ since we want $\tilde{f}$ to be univalent and satisfy properties (97) and (98) for $y = c_3$.

For $x=0$, we are on γ, and for any $y\leq c_3$ and $x=1$, we are on $\tilde{f}\left(\gamma\right)=\tilde{\gamma}=\Omega\cap\tilde{\gamma}'$ and the image of the horizontal line segments for $x\in[0,1]$ in Σ are the line segments joining iy and $\tilde{f}\left(iy\right)$ in Ω.

Now h_1 is $\mathcal{C}^1$ in Σ° as a function of the two real variables (x,y) into $\mathbb{R}^2$ since $\tilde{f}$ is holomorphic. We show that h_1 is a homeomorphism.

Lemma 7.4. *$h_1 : \Sigma^\circ \to \Omega^\circ$ is a homeomorphism.*

Proof. It is enough to prove that H_1 is bijective since continuity follows from $h_1(x,y)$ being $\mathcal{C}^1$.

The function $h_1 : \Sigma^\circ \to \Omega^\circ = h_1(\Sigma^\circ)$ is trivially surjective, so injectivity is all that remains to be proven.

There is a natural parameterization of γ by y, and $\Im\left(\tilde{f}(iy)\right)$ must decrease when y decreases by (98) for all $iy \in \gamma \subset H_2$. Choose any two points z_1 and z_2 in $\partial\Sigma$ such that $\Re(z_1) = 0$ and $\Re(z_2) = 1$ and $\Im(z_1) = \Im(z_2)$. These points are mapped by h_1 respectively to $z \in \gamma$ and $\tilde{f}(z) \in \tilde{f}(\gamma)$, and the horizontal line segment joining z_1 and z_2 is mapped under h_1 onto the line segment which joins z and $\tilde{f}(z)$. This line segment is completely contained in Ω by the above parameterization property. Now the only way h_1 could fail to be injective is if there were two distinct line segments in Σ mapped to two distinct line segments in Ω that intersect at some point in the interior of Ω. This cannot happen due to the above argument of the respective orientations of γ and $\tilde{f}(\gamma)$. $\square$

By calculations identical to those in [Shi00], it can be shown that h_1 has dilatation

$$\left|\frac{\frac{\partial h_1}{\partial \bar{z}}}{\frac{\partial h_1}{\partial z}}\right| < 1/3. \tag{108}$$

Hence, h_1 is a quasi-conformal mapping of Σ° onto the half-strip Ω°, where $h_1^{-1}\left(\tilde{f}(z)\right) = h_1^{-1}(z) + 1$ for $z \in \gamma$.

Set $T(z) = z + 1$. Note that for $iy \in \gamma$ we have $h_1^{-1}\left(\tilde{f}(iy)\right) = h_1^{-1}(iy) + 1$, i.e. the diagram

$$\begin{tikzcd}
\gamma \arrow[r, "h_1^{-1}=id"] \arrow[d, "\tilde{f}"] & \gamma \arrow[d, "T"] \\
\tilde{f}(\gamma) \arrow[r, "h_1^{-1}"] & T(\gamma)
\end{tikzcd} \tag{109}$$

commutes.

Use $h_1 : \Sigma \to \Omega$ to pullback the standard complex structure σ_0 on Ω° to σ on Σ° by $\sigma = h_1^*\sigma_0$. Extend σ to $H_3 \setminus \{z \in \mathbb{C} \mid \Re(z) \in \mathbb{Z}\}$, where $H_3 = \{z \mid \Im(z) < c_3\}$, through further pullback of σ using $T^n(z)$. For any $n \in \mathbb{Z}$,

$$(T^n)^{-1}(\Sigma^\circ) = \{z \in \mathbb{C} \mid \Re(z) \in (]-n, -(n-1)[) \wedge (y < 0)\}. \tag{110}$$

Define σ on $(T^n)^{-1}(\Sigma^\circ)$ by $(T^n)^*\sigma$, i.e.

$$\sigma\Big|_{(T^n)^{-1}(\Sigma^\circ)} = (T^n)^*\left(\sigma\Big|_{\Sigma^\circ}\right). \tag{111}$$

Then extend σ to $\tilde{\sigma}$ on $\mathbb{C}$ by

$$\tilde{\sigma} = \begin{cases} \sigma, & z \in H_3 \setminus \{z \in \mathbb{C} \mid \Re(z) \in \mathbb{Z}\}. \\ \sigma_0, & \text{elsewhere in } \mathbb{C} \end{cases} \tag{112}$$

By construction, $\tilde{\sigma}$ is a T-invariant almost complex structure on $\mathbb{C}$, i.e. $T^*\tilde{\sigma} = \tilde{\sigma}$.

By the measurable Riemann Mapping Theorem, there exists a unique quasiconformal mapping $h_2 : \mathbb{C} \to \mathbb{C}$ such that $h_2^* \sigma_0 = \tilde{\sigma}$ and normalized by fixing $i\tilde{c}$ and $1 + i\tilde{c}$ for some $\tilde{c} < c_3$.

Note that $h_2 \circ T \circ h_2^{-1}$ is a holomorphic bijection

$$(\mathbb{C}, \sigma_0) \xrightarrow{h_2^{-1}} (\mathbb{C}, \tilde{\sigma}) \xrightarrow{T} (\mathbb{C}, \tilde{\sigma}) \xrightarrow{h_2} (\mathbb{C}, \sigma_0) \tag{113}$$

without fixed points, since h_2 is a homeomorphism and T has no fixed points in $\mathbb{C}$. Hence, $h_2 \circ T \circ h_2^{-1}$ is an affine map of the form $z \mapsto z + b$. By the chosen normalization of h_2, we have $h_2 \circ T \circ h_2^{-1} (i\tilde{c}) = h_2 \circ T (i\tilde{c}) = h_2 (1 + i\tilde{c}) = 1 + i\tilde{c}$. Therefore, $b = 1$ so $h_2 \circ T \circ h_2^{-1} = T$.

Define $\Phi = h_2 \circ h_1^{-1}$ on Ω satisfying $\Phi \left(\tilde{f} (z) \right) = \Phi (z) + 1$ on $\gamma = \Omega \cap \gamma'$ respecting the diagram

$$\begin{tikzcd}
\gamma \arrow[r, "h_1^{-1}=id"] \arrow[d, "\tilde{f}"] & \gamma \arrow[r, "h_2"] \arrow[d, "T"] & h_2 (\gamma) \arrow[d, "T"] \\
\tilde{f} (\gamma) \arrow[r, "h_1^{-1}"] & T (\gamma) \arrow[r, "h_2"] & h_2 (\gamma + 1) .
\end{tikzcd} \tag{114}$$

Then Φ is well-defined and homeomorphic on Ω by the properties of h_1 and h_2. Furthermore, Φ is holomorphic on Ω°.

We next extend Φ to $U = interior \left(\bigcup_{n=-2}^{3} \Omega_n \right)$ where $\Omega_n = \tilde{f}^n (\Omega)$ by

$$\Phi (z) = \Phi \left(\tilde{f}^{-n} (z) \right) + n, \quad z \in \Omega_n. \tag{115}$$

Even though the domain U is much larger than we need in order to prove that Φ is holomorphic on γ and $\tilde{f} (\gamma)$, it is chosen in this way so that we have that Φ is univalent in $\{\zeta \mid |\zeta - z| < 5/4 + \epsilon, z \in \Omega\}$ for later use in some deformation estimates (see Section 9). We have that $\Phi (z)$ is well-defined by Equation (115) in $U_1 = U \cap H_4$ where $H_4 = \{z \mid \Im (z) < c_4 = c_3 - 3/4\}$ if there exists a unique integer $-2 \leq n \leq 3$ such that $\tilde{f}^n (z) \in \Omega$ for $z \in U$ (see Figure 32).

Proposition 7.5. *There exists a unique integer* $-2 \leq n \leq 3$ *such that* $\tilde{f}^n (z) \in \Omega$ *for* $z \in U$.

Proof. Consider points z_1 and z_2 in Ω_{n-1} and Ω_n respectively such that $\Im (z_1) = \Im (z_2)$ and connect them by a horizontal line segment intersecting the point z_0 on $\gamma_n = \tilde{f}^n (\gamma)$. The image of this horizontal line segment under $\tilde{f}$ is naturally parameterized by

$$\gamma_n (x) = \tilde{f} (x + iy) , \tag{116}$$

where y is constant. To see how much $\gamma_n (x)$ varies from the horizontal, we calculate

$$|\gamma_n' (x) - 1| = \left| \tilde{f}' (x + iy) - 1 \right| < 1/4, \tag{117}$$

so it follows since $\Re \left(\tilde{f}' \right) > 0$ and $\left| \Im \left(\tilde{f}' \right) \right| < 1/4$ that $\gamma_n (x)$ is contained in the region bounded by the two lines with slope $\pm 1/4$ that intersect at $\tilde{f} (z_0)$, and furthermore, that $\gamma_n (x) |_{\Re(z_1) < x < \Re(z_0)}$ is contained in the left sector and

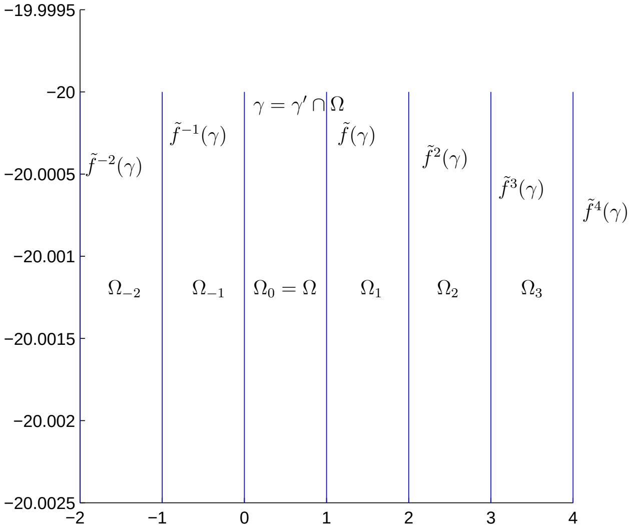

Figure 32: Depiction of the domain U with labelling of the Ω_js and the images of γ. Note that these curves resemble straight lines rather quickly for $\Re(z) \to -2, \ldots, 4$.

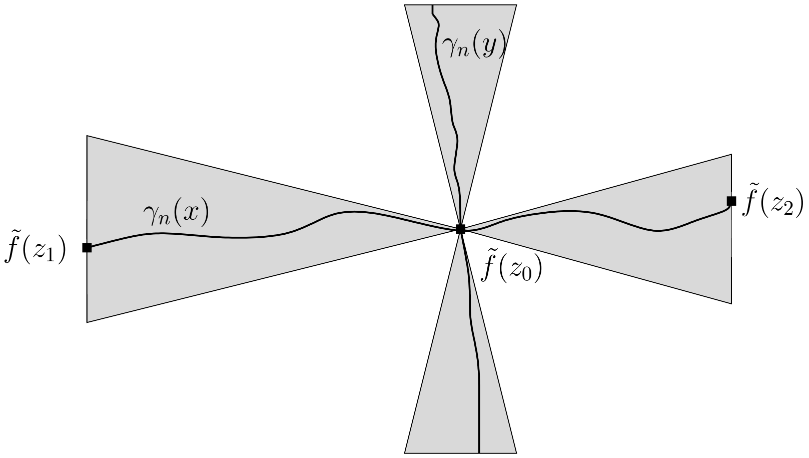

Figure 33: Illustration of the proof of Proposition 7.5

$\gamma_n(x)|_{\Re(z_0)<x<\Re(z_2)}$ is contained in the right sector (see Figure 33). Now to see that $\gamma_n(x)|_{\Re(z_1)<x<\Re(z_0)} \subset \Omega_n$ and $\gamma_n(x)|_{\Re(z_0)<x<\Re(z_2)} \subset \Omega_{n+1}$, we need to show that γ_n, naturally parameterized by $\gamma_n(y) = \tilde{f}^n(iy)$, is contained in the region bounded by the two lines with slope ± 4 that intersect at $\tilde{f}(z_0)$. That is

$$|\gamma_n'(y) - i| < 1/4, \quad n = -2, \ldots, 3. \tag{118}$$

For $n = 1$, we have

$$|\gamma_1'(y) - i| = |\tilde{f}'(iy) - 1| < 1/4, \tag{119}$$

and noticing that

$$\gamma_n'(y) = \tilde{f}'(\gamma_{n-1}(y)) \cdot \gamma_{n-1}'(y), \tag{120}$$

one can show that inequality (118) holds. Since the vertical and horizontal sectors are disjoint, we can conclude that each point $z \in \bigcup_{n=-2}^{3} \Omega_n$ is mapped into $\Omega = \Omega_0$ exactly once by $\tilde{f}^{-n}$, for $-2 \le n \le 3$. $\square$

We have that Φ is holomorphic and univalent in $U \setminus \{\bigcup_j \gamma_j\}$ and is continuous and injective on the γ_j. Therefore, Φ is holomorphic and univalent on all of U as desired by Morera's Theorem.

Let $y_0 < c_4$ be such that the image of the line segment from iy_0 to $\tilde{f}(iy_0)$ under π is completely contained in $\mathbb{C} \setminus \overline{\mathbb{D}}_R$ (see (92)). Define

$$U^*_{[m]} = \pi\left(S \cap \left\{\Im(z) - y_0 < \frac{\Im\left(\tilde{f}(iy_0)\right) - y_0}{\Re\left(\tilde{f}(iy_0)\right)} \Re(z)\right\}\right). \tag{121}$$

The complex structure on $\Phi(\gamma)$ is translation invariant, which allows post-compositon with the map $\exp(-2\pi i(\cdot)) : \Phi(\Omega) \to V^*_{[m]}$, $\eta_{[m]} = \exp(-2\pi i(\cdot)) \circ \Phi \circ \pi^{-1}$, defining the neighborhood $V_{[m]}$ of zero. This defines a chart $\eta_{[m]} : U^*_{[m]} \to V^*_{[m]}$, which can be continuously extended so that $\infty_{[m]} \mapsto 0$.

7.5 Holomorphic Overlap

The images of each connected component of the non-empty intersections $U_1 \cap U_2$ of the open sets in $\mathcal{M}$ defining its charts are subsets of each $V_i = \eta_i(U_i)$, $i = 1, 2$ of one of the following types:

- a strip, half-plane, or vertical half-strip, correspoinding to regular points on $\mathcal{M}$,
- combinations of any two of the above glued along the common bounding separatrix, corresponding to neighborhoods of separatrices on $\mathcal{M}$,
- $\mathbb{D}_{\frac{\sqrt[d-1]{r}}{d-1}}$, corresponding to U_E,
- $V_{[\ell]}$, corresponding to a source or sink,
- $\mathbb{D}$ for a center, or
- $V_{[m]}$ for a multiple equilibrium point.

If V_1, V_2 are one of the first two types, then both $\eta_1 \left(U_1 \cap U_2\right)$ and $\eta_2 \left(U_1 \cap U_2\right)$ are whole strips, planes, or vertical half-strips and

$$\eta_2 \circ \eta_1^{-1} = T, \tag{122}$$

for some translation T.

If V_1 is one of the first two types and $V_2 = \eta_E \left(U_2 = U_E\right)$, then $\eta_1 \left(U_1 \cap U_E\right)$ is a union of at most two half-disks, possibly joined by a common bounding separatrix and

$$\eta_1 \circ \eta_E^{-1} = T \circ z^{d-1}, \tag{123}$$

for some translation T. This is clearly biholomorphic in the domain of definition when the appropriate $d-1^{st}$ branch is chosen.

If $V_1 = V_{[\ell]}$ and $V_2 = \eta_E \left(U_2 = U_E\right)$, then each connected component of $U_1 \cap U_E$ corresponds to exactly two half-disks D_ℓ and $D_{\ell+1}$ joined by part of the common bounding separatrix S_ℓ and

$$\eta_1 \circ \eta_E^{-1} = \varphi_{[\ell]} \circ T \circ z^{d-1}, \tag{124}$$

for some translation T. This is clearly biholomorphic in each connected component of the domain of definition when the appropriate $d-1^{st}$ branches are chosen.

If $V_1 = V_{[k]}$ and $V_2 = V_{[j]}$, then $\eta_1 \left(U_1 \cap U_2\right)$ and $\eta_2 \left(U_1 \cap U_2\right)$ are whole strips (maybe 2 whole strips if $d = 2$), and

$$\eta_2 \circ \eta_1^{-1} = \varphi_{[j]} \circ T \circ \phi_{[k]}^{-1}, \tag{125}$$

for some translation T. The map

$$\phi_{[k]}^{-1} = \frac{\rho_{[k]}}{-2\pi i} \circ \mathcal{L}_{[k]} \tag{126}$$

is well-defined and biholomorphic in the domain of definition, since the logarithm $\mathcal{L}_{[k]} : \tilde{V}_{[k]} \to \Sigma_{[k]}$ taking the head of the logarithmic spiral passing through $z = 1$ to $\frac{-2\pi i}{\rho_{[k]}}\mathbb{R}_+$ is well defined and holomorphic.

If $V_1 = \mathbb{D}$ corresponding to an H-chain $H_{\{[\ell]\}}$, then U_2 must be of one of the first 2 types where $U_1 \cap U_2$ can only correspond to a vertical half-strip and

$$\eta_2 \circ \eta_{\{[\ell]\}}^{-1} = T \circ \frac{\tau_{\{[\ell]\}}}{\mp 2\pi i} \circ \mathcal{L}_0, \tag{127}$$

which is biholomorphic on $\mathbb{D} \setminus [0,1[$ since there is a well-defined and holomorphic branch of the logarithm $\mathcal{L}_0 : \mathbb{D} \setminus [0,1[\to]-\infty, 0[\times]0, 2\pi[$.

If $V_1 = V_{[m]}$ corresponding to a multiple equilibrium point, and V_2 is one of the first 2 types, then at worst $U_1 \cap U_2$ corresponds to part of one of the second types and

$$\eta_{[m]} \circ \eta_2^{-1} = \exp\left(-2\pi i \left(\cdot\right)\right) \circ \Phi \circ \pi^{-1} \circ T, \tag{128}$$

for some translation T, and Φ and π as in Section 7.4. This map is biholomorphic since one can choose a well-defined branch of π^{-1} in the domain of definition, so biholomorphicity of $\exp\left(-2\pi i \left(\cdot\right)\right) \circ \Phi \circ \pi^{-1}$ follows from injectivity and the holomorphic Inverse Function Theorem.

If $V_1 = V_{[m]}$ corresponding to a multiple equilibrium point, and $V_2 = V_{[\ell]}$, then $U_1 \cap U_2$ corresponds to part of exactly one strip and

$$\eta_{[m]} \circ \eta_{[\ell]}^{-1} = \exp\left(-2\pi i\left(\cdot\right)\right) \circ \Phi \circ \pi^{-1} \circ T \circ \phi_{[\ell]}^{-1}, \tag{129}$$

for some translation T. This map is biholomorphic on its domain of definition by the previous arguments for $\exp\left(-2\pi i\left(\cdot\right)\right) \circ \Phi \circ \pi^{-1}$ and $\phi_{[\ell]}^{-1}$. Therefore, we have made an atlas with holomorphic overlap covering $\mathcal{M}$, and we can conclude that $\mathcal{M}$ is a Riemann surface.

8 $\mathcal{M}$ isomorphic to $\hat{\mathbb{C}}$

Proposition 8.1. *$\mathcal{M}$ is homeomorphic to $\hat{\mathbb{C}}$.*

Proof. We utilize the Euler characteristic. Note that $\mathcal{M}$ has a topology induced by the topology of $\mathbb{C}$. The end E gives one vertex, and all other equilibrium points apart from centers contribute a vertex. That is, there are a total of $1 + d - c - \frac{p_P}{2}$ vertices. The number of edges is $2\left(d-1\right) - h$, the number of separatrices. Each strip gives one face, each basin of a center gives one face, and each upper and lower half-plane gives a face. That is, altogether we have $s + c + 2\frac{p_P}{2}$ faces. In total,

$$\begin{aligned}\chi\left(\mathcal{M}\right) &= \left(1 + d - c - \frac{p_P}{2}\right) - \left(2\left(d-1\right) - h\right) + \left(s + c + 2\frac{p_P}{2}\right)\\ &= 1 - d + 2 + h + s + \frac{p_P}{2}\\ &= 2 \end{aligned} \tag{130}$$

since $s = d - 1 - \frac{p_P}{2} - h$ (see Equation 61). Therefore, $\mathcal{M}$ is homeomorphic to $\hat{\mathbb{C}}$. ☐

Corollary 8.2. *$\mathcal{M}$ is isomorphic to $\hat{\mathbb{C}}$.*

Proof. Since $\mathcal{M}$ is a simply connected Riemann surface that is compact, we have that it must be conformally equivalent to the Riemann sphere $\hat{\mathbb{C}}$ by The Uniformization Theorem. ☐

We now analyze the vector field $\xi_{\mathcal{M}}$ on $\mathcal{M}$.

9 The Associated Vector Field $\xi_{\mathcal{M}}$

For $U_{[\ell]}$ such that $[\ell]$ is an odd or even equivalence class, the vector field $\xi_{\mathcal{M}}$ is defined on $U_{[\ell]}^*$ by $\left(\eta_{[\ell]}\right)_*\left(\xi_{\mathcal{M}}\right) = \left(\varphi_{[\ell]}\right)_*\left(\frac{d}{dz}\right)$. On $\Sigma_{[\ell]} \cup \left\{\mathbb{R}_\pm \cup \left(\rho_{[\ell]} + \mathbb{R}_\pm\right)\right\}$, there is a constant vector field $\frac{d}{dz}$ that conjugates by $\varphi_{[\ell]}$ to the linear vector field $\frac{\mp 2\pi i}{\rho_{[\ell]}} z \frac{d}{dz}$ in $V_{[\ell]} \backslash \{0\}$. For $[\ell]$ odd, the puncture $-\infty_{[\ell]} \in \mathcal{M}$ corresponds to a sink with multiplier $\frac{-2\pi i}{\rho_{[\ell]}}$, and for $[\ell]$ even, the puncture $+\infty_{[\ell]} \in \mathcal{M}$ corresponds to a source with multiplier $\frac{2\pi i}{\rho_{[\ell]}}$. We see this by observing that

$$\left(\eta_E\right)_*\left(\xi_{\mathcal{M}}\right) = \left(\varphi_{[\ell]}\right)_*\left(\frac{d}{dz}\right) = \frac{\mp 2\pi i}{\rho_{[\ell]}} z \cdot \frac{d}{dz} \tag{131}$$

since $\frac{\mp 2\pi i}{\rho_{[\ell]}}\varphi_{[\ell]}(z) = \frac{d}{dz}\varphi_{[\ell]}(z)$. The map $\varphi_{[\ell]}$ extends holomorphically to $V_{[\ell]}$ by taking the value 0 at $z = 0$. Hence, $\xi_{\mathcal{M}}$ extends holomorphically to the puncture $\infty_{[\ell]}$ by $\xi_{\mathcal{M}} = 0$.

For $U_{\{[\ell]\}}$ corresponding to a closed H-chain $H_{\{[\ell]\}}$, we define the vector field $\xi_{\mathcal{M}}$ on $U^*_{\{[\ell]\}}$ by $\left(\eta_{\{[\ell]\}}\right)_*(\xi_{\mathcal{M}}) = \left(\varphi_{\{[\ell]\}}\right)_*\left(\frac{d}{dz}\right)$. On the vertical half-strips $C_{\{[\ell]\}}$, there is a constant vector field $\frac{d}{dz}$ that conjugates by $\varphi_{[\ell]}$ to the linear vector field $\frac{\mp 2\pi i}{\tau_{\{[\ell]\}}} z \frac{d}{dz}$ in $\mathbb{D}^*$. The puncture corresponds to a center with multiplier $\frac{\mp 2\pi i}{\tau_{\{[\ell]\}}}$. The map $\varphi_{\{[\ell]\}}$ extends holomorphically to $\mathbb{D}$ by taking the value 0 at $z = 0$. Hence, $\xi_{\mathcal{M}}$ extends holomorphically to the puncture $\infty_{\{[\ell]\}}$ by $\xi_{\mathcal{M}} = 0$.

The induced vector field in a neighborhood of E can be calculated:

$$(\eta_E)_*(\xi_{\mathcal{M}}) = (\phi_E)_*\left(\frac{d}{dz}\right) = \frac{1}{d-1} w^{-(d-2)} \frac{d}{dw} \tag{132}$$

in $\mathbb{D}^*_{\frac{d-1\sqrt{r}}{d-1}}$ since the $d-1$ covering of $\mathbb{D}^*_r$ has constant vector field $\frac{d}{dz}$. Therefore, the vector field $\xi_{\mathcal{M}}$ has a pole of order $d-2$ at E.

For $U_{[m]}$ corresponding to a mixed equivalence class $[m]$, we wish to show that the vector field in the chart $\eta_{[m]} : U^*_{[m]} \to V^*_{[m]}$ is of order $\mathcal{O}\left(z^{p[m]/2+1}\right)$ in $V^*_{[m]}$, a neighborhood of zero. That is, we will show $\infty_{[m]} \in \mathcal{M}$, corresponding to the puncture in $U^*_{[m]}$ is a multiple equilibrium point of multiplicity $p_{[m]}/2+1$ for $\xi_{\mathcal{M}}$.

We will use Koebe's Distortion Theorem and the extension of Φ from Section 7.4 to prove the following lemma that $\Phi'(z)$ is uniformly bounded in V.

Lemma 9.1. *Suppose we have Φ as above in U. Then there exist constants k_1 and k_2 in $\mathbb{R}_+$ such that*

$$k_1 < |\Phi'(z)| < k_2, \quad z \in V. \tag{133}$$

We first need to use a modified version of Koebe's Distortion Theorem. It is stated in [Pom75], for functions univalent in $\mathbb{D}$ and of the form $g(z) = z + a_2 z^2 + \ldots$,

$$\frac{|z|}{(1+|z|)^2} \le |g(z)| \le \frac{|z|}{(1-|z|)^2}. \tag{134}$$

This is restricted to functions with $g(0) = 0$ and $g'(0) = 1$ defined in $\mathbb{D}$ which we want to extend to functions univalent in a disk $\mathbb{D}_R(z_0)$ centered at z_0 with radius R. We show that if f is univalent in $\{z \mid |z - z_0| < R\}$ then

$$\frac{|z-z_0|/R}{(1+|z-z_0|/R)^2} \le \frac{|f(z) - f(z_0)|}{|Rf'(z_0)|} \le \frac{|z-z_0|/R}{(1-|z-z_0|/R)^2}. \tag{135}$$

This is true by the following. Let $h : \{|\tilde{z} - f(z_0)| < Rf'(z_0)\} \to \mathbb{D}$, $h(\tilde{z}) = \frac{\tilde{z} - f(z_0)}{Rf'(z_0)}$ and note that the mapping $z \mapsto \frac{z - z_0}{R}$ maps the disk centered at z_0 and with radius R to the disk $\mathbb{D}$. Let $g : \mathbb{D} \to \mathbb{D}$ be defined by $g(w) = h(f(Rw + z_0))$. This is the composition of univalent functions, so g is univalent. Furthermore, $g(0) = 0$ and $g'(0) = 1$, so g must take the form $g(w) = w + h.o.t$, and hence by Koebe's Distortion Theorem,

$$\frac{|w|}{(1+|w|)^2} \le \frac{|f(Rw + z_0) - f(z_0)|}{|Rf'(z_0)|} \le \frac{|w|}{(1-|w|)^2}. \tag{136}$$

Remembering that $w = \frac{z-z_0}{R}$ gives the result.

Proof of Lemma 9.1. It follows from the above that for some $z \in V$, if Φ is univalent in $\{\zeta \mid |\zeta - z| < R\}$, where $\zeta = z + v(z) = \tilde{f}(z)$, then

$$\frac{|v(z)|}{(1 + |v(z)|/R)^2} \leq \frac{|\Phi(z + v(z)) - \Phi(z)|}{|\Phi'(z)|} \leq \frac{|v(z)|}{(1 - |v(z)|/R)^2}, \tag{137}$$

and hence

$$\frac{(1 - |v(z)|/R)^2}{|v(z)|} \leq |\Phi'(z)| \leq \frac{(1 + |v(z)|/R)^2}{|v(z)|}. \tag{138}$$

From the condition $|v(z) - 1| < 1/4$, we have $3/4 < |v(z)| < 5/4$, and to have $|\Phi'|$ bounded away from 0 and ∞, we need therefore $R \geq 5/4 + \epsilon$. Since Φ is univalent in U, we have

$$\frac{(2/5 + \epsilon_1)^2}{5/4} < |\Phi'(z)| < \frac{(2 - \epsilon_2)^2}{3/4} \tag{139}$$

satisfied for all $z \in V \cap \{z \mid \Im(z) < c_4 - (5/4 + \epsilon)\}$. □

We next examine the vector field in $U^*_{[m]}$ to determine what form $\xi_{\mathcal{M}}$ takes at $\infty_{[m]}$. We will show that $\left(\eta_{[m]}\right)_* (\xi_{\mathcal{M}}) = o(z)$ for $z \in V^*_{[m]}$.

From $\pi_* \left(j \frac{d}{dz}\right) = \frac{d}{dw}$, the vector field $j \frac{d}{dz}$ in S is expressed by

$$j(z) = \frac{1}{\pi i p_{[m]} \exp\left(\pi i p_{[m]} z\right)}. \tag{140}$$

The expression of the vector field $g \frac{d}{dz}$ in Φ coordinates is determined by

$$g(\Phi(z)) = \Phi'(z) j(z). \tag{141}$$

Now by Lemma 9.1 $|\Phi'|$ is bounded away from 0 and ∞, then

$$\Phi'(z) j(z) = \mathcal{O}(j(z)) = \mathcal{O}\left(\exp\left(-\pi i p_{[m]} z\right)\right). \tag{142}$$

Now under the map $\exp(-2\pi i w)$, the vector field $f \frac{d}{dz}$ in the punctured disk is determined by

$$f(\exp(-2\pi i w)) = -2\pi i \exp(-2\pi i w) g(w) = \mathcal{O}\left(\exp\left(-2\pi i (w + \left(p_{[m]}/2\right) z)\right)\right), \tag{143}$$

which gives that $f = o(z)$ in the punctured disk. Hence, $\left(\eta_{[m]}\right)_* (\xi_{\mathcal{M}}) = o(z) \frac{d}{dz}$, where the puncture at 0 in $V^*_{[m]}$ corresponds to the puncture in $U^*_{[m]}$ which can be uniquely extended to $U_{[m]}$ by addition of the point $\infty_{[m]}$. The vector field $\xi_{\mathcal{M}}$ can be extended holomorphically to $\infty_{[m]}$, i.e. such that $\left(\eta_{[m]}\right)_* (\xi_{\mathcal{M}}) = 0 \frac{d}{dz}$ at 0 in $V_{[m]}$.

Now we show that the multiplicity of the zero is in fact $\left(p_{[m]}/2 + 1\right)$. We do this by an index argument. Consider the (piecewise smooth) Jordan curve about $\infty_{[m]}$ in $U_{[m]}$ that corresponds to the curve $\gamma_{[m]}$ in rectifying coordinates with half-circles in each upper and lower half-plane and appropriate line segments in the half-strips with clockwise orientation so that $\infty_{[m]}$ is to the left of the curve (see Figure 34). The curve $\gamma_{[m]}$ maps to another Jordan curve γ in $V^*_{[m]}$

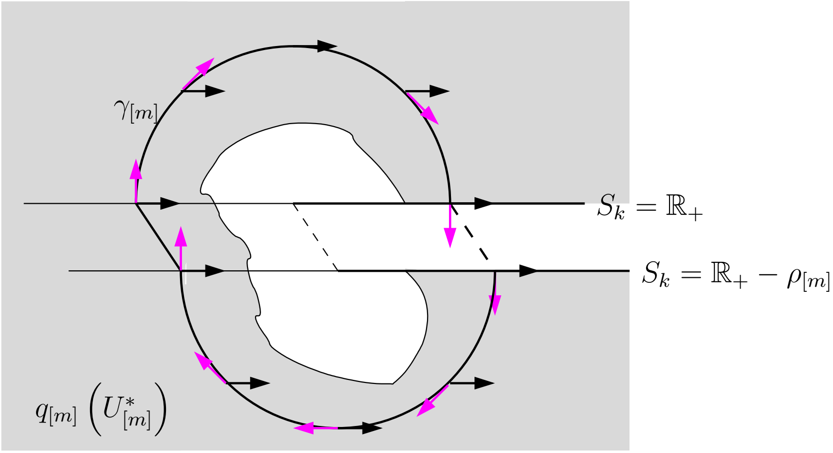
$\gamma_{[m]}$
$S_k = \mathbb{R}_+$
$S_k = \mathbb{R}_+ - \rho_{[m]}$
$q_{[m]}\left(U^*_{[m]}\right)$

Figure 34: Possible depiction of $q_{[m]}\left(U^*_{[m]}\right)$ in rectifying coordinates (shaded area) with $p_{[m]} = 2$ and $\Im\left(\rho_{[m]}\right) > 0$. The vector field $\frac{d}{dz}$ is tangent to the curve $\gamma_{[m]}$ in exactly $p_{[m]}$ places. Compare with Figure 35.

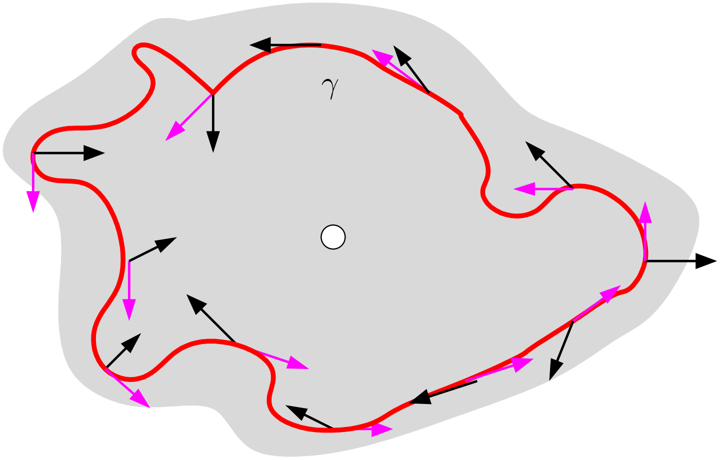

Figure 35: Possible depiction of the index of $\left(\eta_{[m]}\right)_*(\xi_{\mathcal{M}})$ in a neighborhood of zero where the multiplicity of $\infty_{[m]}$ is 2. The light vectors are tangent vectors to γ, and the black vectors belong to the vector field at points along γ. Notice that the vector field is tangent to γ exactly twice: once pointing in the same direction as the tangent vector and once against. Compare with Figure 34.

under $\eta_{[m]}$ since $\eta_{[m]}$ is univalent. Moreover, $\left(\eta_{[m]}\right)_*(\xi_{\mathcal{M}})$ is never 0 along γ. The angles between $\left(\eta_{[m]}\right)_*(\xi_{\mathcal{M}})$ on γ and the tangent vectors of γ are the same as the angles between the vector field $\frac{d}{dz}$ and the tangent vectors of $\gamma_{[m]}$ since $\eta_{[m]}$ is conformal (see Figure 35). This implies that on γ, $\left(\eta_{[m]}\right)_*(\xi_{\mathcal{M}})$ will be tangent to γ exactly $p_{[m]}$ times, and alternating with pointing along the orientation of γ and against the orientation of γ when we travel along γ. Along the orientation of γ, on the arcs between the tangents going along to the tangents going against, the vector field must be pointing inward, since this corresponds to what happens in rectifying coordinates. This implies that the vector field must be rotating in the same orientation as γ, otherwise there would be a place in this arc where there is another tangent. So with respect to the tangents of γ, $\left(\eta_{[m]}\right)_*(\xi_{\mathcal{M}})$ has rotated $+p_{[m]}/2$ times. We must add one more time around, accounting for the index of γ. This gives that $\left(\eta_{[m]}\right)_*(\xi_{\mathcal{M}})$ has index $p_{[m]}/2+1$ at 0.

We have that $\xi_{\mathcal{M}}$ is holomorphic on $\mathcal{M}\setminus\{E\}$ since it can be expressed as $g\frac{d}{dz}$ where g is holomorphic in the domain of each chart.

10 Proof of the Structure Theorem

We now show that there is a unique conformal isomorphism $\Phi:\mathcal{M}\to\hat{\mathbb{C}}$ that induces the vector field $\xi_P\in\Xi_d$ having the given invariants.

Theorem 10.1. *There exists a unique conformal isomorphism* $\Phi:\mathcal{M}\to\hat{\mathbb{C}}$ *such that* $\Phi(E)=\infty$ *and such that* $\Phi_*(\xi_{\mathcal{M}})=\xi_P$ *where* $\xi_P\in\Xi_d$ *and* ξ_P *has the given invariants.*

Proof. By the Uniformization Theorem, there exists an isomorphism $\Psi:\mathcal{M}\to\hat{\mathbb{C}}$, which is unique up to post composition by a Möbius transformation and induces a vector field $\Psi_*(\xi_{\mathcal{M}})$ defined on $\hat{\mathbb{C}}$. Choose Ψ such that $\Psi(E)=\infty$. Then $\Psi_*(\xi_{\mathcal{M}})$ is a holomorphic vector field on $\mathbb{C}$, expressed in canonical coordinates as $g\frac{d}{dz}$. We know g has a unique pole of order $d-2$ at ∞ since $(\eta_E)_*(\xi_{\mathcal{M}})=\frac{-1}{z^{d-2}}\frac{d}{dz}$ for $z\in V_0$.

Lemma 10.2. *If* $g\frac{d}{dz}$ *is holomorphic in* $\mathbb{C}$ *and* $g\frac{d}{dz}$ *has a pole of order* $d-2$ *at* ∞*, then* $g\frac{d}{dz}$ *is a polynomial vector field of degree* d*.*

Proof. Since g is entire, it admits a Taylor series expansion

$$g(z)=\sum_{n=0}^{\infty}a_nz^n,\quad z\in\mathbb{C}. \tag{144}$$

To examine the behavior near ∞, we need to make a transformation by $w=\varphi(z)=\frac{1}{z}$ using the transformation rule for vector fields

$$\tilde{g}(w)=\left(-w^2\right)\sum_{n=0}^{\infty}a_n\left(\frac{1}{w}\right)^n,\quad w\in\mathbb{C}^*. \tag{145}$$

So if $\tilde{g}\frac{d}{dw}$ has a pole of order $d-2$ at $w=0$, then $a_n=0$ for $n>d$, $a_d\neq 0$, and it follows that g is a polynomial of degree d. □

If g has leading coefficient a_d, then for $A = \sqrt[d-1]{a_d}$, $g\frac{d}{dz}$ is conjugate to a monic polynomial vector field whose incoming separatrices have asymptotic directions $\delta_j = \exp\left(2\pi i \frac{j}{2(d-1)}\right)$ where $j \in \{0, 2, \ldots, 2d-4\}$. We choose A such that $A\Psi(S_0)$ is asymtotic to $\mathbb{R}_+$ near infinity[3]. We choose B such that

$$\sum_{H_{\{[\ell]\}} \subset H} \left(\Psi\left(\infty_{\{[\ell]\}}\right) + B\right) + \sum_{[\ell] \subset L} \left(p_{[\ell]}/2 + 1\right)\left(\Psi\left(\infty_{[\ell]}\right) + B\right) = 0, \tag{146}$$

centering the equilibrium points. Let

$$\sum_{H_{\{[\ell]\}} \subset H} \Psi\left(\infty_{\{[\ell]\}}\right) + \sum_{[\ell] \subset L} \left(p_{[\ell]}/2 + 1\right)\Psi\left(\infty_{[\ell]}\right) = \tilde{c}. \tag{147}$$

If $\tilde{c} = 0$, we are finished. If $\tilde{c} \neq 0$, then Equation (146) gives the equation $\tilde{c} + dB = 0$, giving $B = \frac{-\tilde{c}}{d}$. Let $\tilde{A}$ be the unique affine map with A and B as described above. Then $\Phi = \tilde{A} \circ \Psi$ is the unique isomorphism conjugating $g\frac{d}{dz}$ to a monic, centered polynomial vector field $P\frac{d}{dw}$ of degree d.

The combinatorial invariant is preserved since Φ is a conformal isomorphism such that $s_0 = \Phi(S_0)$ has $\mathbb{R}_+$ as asymptote.

The vector fields $\xi_{\mathcal{M}}$ and $\Phi_*\left(\xi_{\mathcal{M}}\right) = P\frac{d}{dw}$ must have the same number of zeros with the same multiplicities (and at the images $\Phi\left(\infty_{[\ell]}\right)$ and $\Phi\left(\infty_{\{[\ell]\}}\right)$) and the same dynamical residues (see, for example, Theorem 1 in [BT76]), hence the same analytic invariants.

Therefore, $(\sim_P, H_P) = (\sim, H)$, and $A\left(\xi_P\right) = A\left(\xi_{\mathcal{M}}\right)$ as desired. $\square$

References

[AGP09] M.J. Álvarez, A. Gasull, and R. Prohens. Topological classification of polynomial complex differential equations with all the critical points of center type. Preprint, 2009.

[BC06] Xavier Buff and Arnaud Chéritat. Quadratic julia sets with positive area. *arXiv:math/0605514v2*, 2006, 0605514v2.

[Ben91] Harold E. Benzinger. Plane autonomous systems with rational vector fields. *Transactions of the American Mathematical Society*, 326(2):465–484, 1991.

[Ben93] Harold E. Benzinger. Julia sets and differential equations. *Proceedings of the American Mathematical Society*, 117(4):939–946, 1993.

[BT76] Louis Brickman and E. S. Thomas. Conformal equivalence of analytic flows. *Journal of Differential Equations*, 25:310–324, 1976.

[BT07] Xavier Buff and Tan Lei. Dynamical convergence and polynomial vector fields. *Journal of Differential Geometry*, 77(1):1–41, 2007.

[DES] Adrien Douady, Francisco Estrada, and Pierrette Sentenac. Champs de vecteurs polynomiaux sur $\mathbb{C}$. Unpublished manuscript.

---

[3] See Remark 2.5.

[DT] Kealey Dias and Tan Lei. Parameter space of complex polynomial vector fields in $\mathbb{C}$. In preparation.

[Eps] Adam Lawrence Epstein. Parabolic bifurcations in conformal dynamics (notes).

[GGJ04] Antonio Garijo, Armengol Gasull, and Xavier Jarque. Normal forms for singularities of one dimentional holomorphic vector fields. *Electronic Journal of Differential Equations*, 2004(122):1–7, 2004.

[Jen58] J.A. Jenkins. *Univalent Functions*. Springer-Verlag, 1958.

[LS04] Jaume Llibre and Dana Schlomiuk. The geometry of quadratic differential systems with a weak focus of third order. *Canad. J. Math.*, 56(2):310–343, 2004.

[MR02] Jesús Muciño-Raymundo. Complex structures adapted to smooth vector fields. *Mathematische Annalen*, 322:229–265, 2002.

[Nee94] D.J. Needham. On meromorphic complex differential equations. *Dynamics and Stability of Systems*, 9:99–121, 1994.

[Oud99] R. Oudkerk. *The Parabolic Implosion for* $f_0(z) = z + z^{\nu+1} + O(z^{\nu+2})$. PhD thesis, University of Warwick, 1999.

[Pom75] Christian Pommerenke. *Univalent Functions*. Vandenhoeck and Ruprecht, Göttingen, 1975.

[Shi00] Mitsuhiro Shishikura. Bifurcation of parabolic fixed points. In Tan Lei, editor, *The Mandelbrot Set, Theme and Variations*. Cambridge University Press, London, 2000.

[Str84] Kurt Strebel. *Quadratic Differentials*. Springer-Verlag, 1984.

[Sve78] Ronald Sverdlove. Vector fields defined by complex functions. *Journal of Differential Equations*, 34:427–439, 1978.

[Sve81] Ronald Sverdlove. Inverse problems for dynamical systems. *Journal of Differential Equations*, 42:72–105, 1981.

Department of Mathematics
Technical University of Denmark
Building 303S
2800 Kgs. Lyngby, Denmark

e-mail: B.Branner@mat.dtu.dk
e-mail: K.Dias@mat.dtu.dk